Quantifying closed-basin lake temperature and hydrology by inversion of oxygen isotope and trace element paleoclimate records

Daniel E. Ibarra[*, †] and C. Page Chamberlain[*]

[*] Department of Earth System Science, 473 Via Ortega, Rm. 140, Stanford University, Stanford, California 94305-4216, USA

[†] Corresponding Author: Address: Department of Earth System Science, 473 Via Ortega, Rm. 140, Stanford University, Stanford, California 94305-4216, USA; Email: danieli@stanford.edu

ABSTRACT. Lake systems are important paleoclimate archives that preserve ecosystem and hydrologic responses to critical periods in Earth history, such as carbon cycle perturbations and glacial-interglacial cycles. Geochemical measurements of biogenic carbonate (for example, $\delta^{18}O$, $\delta^{13}C$, $^{87}Sr/^{86}Sr$, [Li], [U], [Sr], and [Mg]) are indicators of hydrologic variability in lake systems throughout the geologic record. In this study, we present a new closed-basin lake modeling approach, HyBIM (the Hydrologic Balance Inverse Model), that employs a system of total differential equations and uses the measured $\delta^{18}O$, Sr/Ca, and Mg/Ca of biogenic carbonate to determine changes in temperature, runoff, and lake evaporation. Using equally-spaced time steps, these equations are simultaneously solved to constrain the hydrologic parameters of the lake as recorded in biogenic carbonate. We use a Monte Carlo approach to account for uncertainty in the input parameters, such as $\delta^{18}O$ temperature relationships, partition coefficient uncertainty, and watershed solute chemistry.

For illustrative purposes, we apply the model to two ostracod valve datasets covering different timescales: (1) the Cretaceous Songliao Basin, northeast China, and (2) Holocene Lake Miragoane, Haiti. Modern water measurements of water isotopes and cation concentrations from each location are required as model inputs. We compare our modeling results with author interpretations and geologic observations. The modeling approach presented in this study can be applied to other closed-basin lake records, can be modified for other calcifying species (for example, gastropods or mollusks) or with calibration to inorganic lacustrine carbonate. In addition, this approach holds promise for extension with additional proxy measurements (that is, δD, U/Ca or Li/Ca) and changing source area on tectonic timescales using proxies that reflect changing source lithology (that

is, Sr and Pb isotopes). Future incorporation of age model uncertainty in the Monte Carlo approach will also provide utility by quantifying temporal uncertainty on the hydrologic response recorded by lake sediments.

Keywords: lakes, paleohydrology, inverse model, trace elements, oxygen isotopes

INTRODUCTION

Lake systems provide valuable paleoclimate archives as natural integrators of terrestrial processes. Lake deposits from hydrologically closed basins or terminal lakes record important changes in climate, human activity, hydrology, ecology, and tectonics (Antevs, 1948; Eugster and Jones, 1979; Currey, 1990; Binford and others, 1997; Carroll and Bohacs, 1999; Reheis, 1999; Demko and others, 2005; Horton and Chamberlain, 2006; Davis and others, 2009; Reheis and others, 2014; Hillman and others, 2014; Smith and others, 2014). Additionally, lake sediments provide the most widely available and continuous records of terrestrial climate available to reconstruct past climate (for example, Oviatt and McCoy, 1992; Colman and others, 1995; Williams and others, 1997; Bohacs et al., 2003; Melles and others, 2012). Accurate estimates of past precipitation, runoff, and/or temperature are important for studying the evolution of landscapes and the diversification and migration of species, as well as to test climate model predictions of past climate (for example, Rozanski and others, 1997; Partridge and others, 1997; Steinman and others, 2012; Ibarra and others, 2014).

Studies of ancient lake systems have long sought to infer climate conditions leading to the existence and persistence of lakes in terrestrial settings. Inferring the climatic setting and the open versus closed hydrology of a lake system using facies identification has been extensively

57 investigated (for example, Nilsson, 1931; Eugster and Kelts, 1983; Kelts, 1988; Talbot, 1990;
58 Carroll and Bohacs, 1999). Within the Carroll and Bohacs (1999) framework, closed-basin lakes
59 are of two types: balanced-fill and underfilled. Underfilled lake systems are identified by
60 evaporative facies (Jones and others, 1977; Eugster and Jones, 1979; Horita, 1990) and are
61 typical of many Quaternary playa-lake systems found in semi-arid regions of the mid-latitudes,
62 such as the western United States (Mifflin and Wheat, 1979; Reheis and others, 2014). In
63 contrast, balanced-filled lake systems are typical of freshwater to saline conditions with mixed
64 carbonate and siliciclastic sediments (for example, Carrol, 1998; Kempf and others, 2009;
65 Doebbert and others, 2014).
66 For closed-basin Quaternary lake systems, in which tectonic rearrangement is negligible,
67 climatic conditions have been quantified using measures of lake surface area and tributary size
68 (Snyder and Langbein, 1962; Mifflin and Wheat, 1979; Bowler, 1981; Benson and Paillet, 1989;
69 Bengtsson and Malm, 1997; Reheis, 1999; Sack, 2009; Broecker, 2010; Munroe and Laabs,
70 2013; Hudson and Quade, 2013; Ibarra and others, 2014; Huth and others, 2015; Hudson and
71 others, 2015). Additionally, recent work modeling stable isotopes in closed-basin balance-filled
72 lakes takes advantage of longer (relative to overfilled/open lakes) residence times to infer
73 climatic conditions by relating the $\delta^{18}O$ or δD to the hydrologic balance (Horita, 1990; Hostetler
74 and Benson, 1994; Benson and White, 1994; Gibson and others, 2002; Gibson and Edwards,
75 2002; Benson and Paillet, 2002; Jones and others, 2007; Russell and Johnson, 2006; Jones and
76 Imbers, 2010; Doebbert and others, 2010; Steinman and others, 2010a,b; 2012; 2013; Steinman
77 and Abbott, 2013; Jasechko and others, 2013; Stansell and others, 2013; Ibarra and others, 2014;
78 Jasechko and others, 2014; Gibson and others, 2015). Fundamental to applying an isotopic
79 modeling approach are assumptions concerning the watershed precipitation-runoff relationships

(Jones and others, 2007; Ibarra and others, 2014), mixing or stratification of the lake (Imberger and Ivey, 1991), basin-scale and regional vapor recycling (Gat and Matsui, 1991; Gat and others, 1994; Burnett and others, 2003; Winnick and others, 2014), and groundwater influences (Krabbenhoft and others, 1990a,b; Shapley and others, 2005; Guay and others, 2006; Steinman and others, 2013). While these models offer powerful methods to reconstruct the hydrology of lake systems they are limited by the numerous input parameters required that are difficult to constrain in ancient lake systems. Another approach, outlined here, is to use additional measurements, such as trace elements, that can be meaningfully related to climatic conditions and will reduce the assumptions necessary for accurate, quantitative climatic reconstructions. Using trace element and oxygen isotope measurements it is then possible to tightly constrain the system using far fewer input parameters.

In this paper, we develop a new modeling framework exploiting variations in $\delta^{18}O$ and trace elements (Mg and Sr) measured in lacustrine carbonates and utilizing a series of total differential equations. We apply this model to previously published ostracod paleoclimate records for closed basins. Lacustrine ostracod records are used here for illustrative purposes because of their broad paleoclimate applications in historical (for example, Engstrom and Nelson, 1991; Holmes and others, 2007a; Zhang and others, 2009), Quaternary (for example, Edney and others, 1990; Hodell and others, 1991; Curtis and Hodell, 1993; Lamb and others, 1999; Cohen and others, 2000; Holmes and others, 2007b; Gouramanis and others, 2010), and deep-time (for example, Forester, 1991; Chamberlain and others, 2013) settings. Extensive work has also been carried out on the ecology, taphonomy, and taxonomy of ostracod species (for example, Horne and others, 2002; Frogley and others, 2002; Bennett and others, 2011; Blome and others, 2014), and modern ostracod datasets have been extensively studied and provide the necessary empirical

103 calibrations of trace element distribution coefficients and vital effects (for example, Engstrom
104 and Nelson, 1991; Xia and others, 1997a,b; Wansard and others, 1998; De Deckker and others,
105 1999; Dettman and others, 2002; Holmes and Chivas, 2002; Dwyer and others, 2002; Ito and
106 Forester, 2009; Gouramanis and De Deckker, 2010; Marco-Barba and others, 2012; Börner and
107 others, 2013) necessary to constrain our model. The modeling framework presented in this paper
108 applies, given the existence of relevant and accurate calibrations, to any biogenic carbonate
109 records from a closed-basin lake setting.
110
111 MODEL DEVELOPMENT
112 We present the Hydrologic Balance Inversion Model (HyBIM), an inverse model using a
113 system of total differential equations that are inverted to solve for the extensive variables in lake
114 chemistry. The structure of the model is similar to models that quantify changes in the global
115 carbon cycle and/or other biogeochemical cycles as recorded in marine sediments (for example,
116 Goddéris and François, 1996; Derry and France-Lanord, 1996; François and Goddéris, 1998; Li
117 and others, 2009; Li and Elderfield, 2013). We solve for the relative changes in temperature and
118 lake volume, and thus rely only on the first derivative of the input dataset and not the absolute
119 value of the isotopic and trace element measurements. Because of this formulation order of
120 magnitude fluctuations in lake volume cannot be modeled by this approach. Fundamentally, this
121 model quantifies the observations made by previous studies that qualitatively employed end-
122 member mixing (from a fresh source to an evaporative lake) in closed-basin lacustrine deposits
123 based on the covariance of Sr/Ca, Mg/Ca, $\delta^{18}O$ and $\delta^{13}C$ (for example, Müller and others, 1972;
124 Eugster and Kelts, 1983; Talbot, 1990; Li and Ku, 1997; Garnett and others, 2004; Davis and
125 others, 2009; Horton and Oze, 2012; McGee and others, 2012; Chamberlain and others, 2013;

126 Horton and others, 2015). We do not incorporate variations in $\delta^{13}C$ in this initial iteration of
127 HyBIM; however, evaporative processes and lake residence times should also control the
128 systematics of the $\delta^{13}C$ of carbonates from terminal lake systems (see discussion in Horton and
129 others, 2015).

130 First, we establish the modeling framework using a system of total differential equations.
131 Second, we describe the Monte Carlo routine used to account for parameter and input data
132 uncertainty (for example, Fantle, 2010; Royer and others, 2014). Third, we discuss the input
133 dataset (the time series of measurements) and necessary input parameters. Finally, we describe
134 the quantification of the partial derivatives necessary to constrain the model and necessary input
135 parameters. This model is available as a generic R code built for input of data from any time
136 series of biogenic carbonate from the authors website (http://paleoclimate.stanford.edu). For
137 illustrative purposes, we apply HyBIM to two ostracod valve datasets covering different
138 timescales: (1) the Cretaceous Songliao Basin, northeast China, and (2) Holocene Lake
139 Miragoane, Haiti. All model parameters are summarized in table 1 and a schematic of the model
140 structure is presented in figure A1.

141 *Model Framework*

142 Here, we present a modeling framework that produces a time series of temperature
143 changes, effects of evaporation, and relative volume estimates for runoff for carbonate-bearing
144 (here ostracods) paleolake records. Chivas and others (1986a) previously suggested a
145 quantitative framework by which a unique solution for paleotemperature and paleosalinity could
146 be calculated using paired Mg/Ca and $\delta^{18}O$ measurements. Following this observation, we write
147 three total differential equations for lake water that describe the effects of temperature,
148 evaporation, and runoff/precipitation on the oxygen isotopic and trace element concentration of

ostracods in a hydrologically closed lake. The three total differential equations (for lake water $\delta^{18}O$, [Mg], and [Sr]) are:

$$d(\delta^{18}O) = \left(\frac{\partial(\delta^{18}O)}{\partial T}\right)dT + \left(\frac{\partial(\delta^{18}O)}{\partial F_{evap}}\right)dF_{evap} + \left(\frac{\partial(\delta^{18}O)}{\partial F_{input}}\right)dF_{input} \quad (1)$$

$$d[Sr] = \left(\frac{\partial[Sr]}{\partial T}\right)dT + \left(\frac{\partial[Sr]}{\partial F_{evap}}\right)dF_{evap} + \left(\frac{\partial[Sr]}{\partial F_{input}}\right)dF_{input} \quad (2)$$

$$d[Mg] = \left(\frac{\partial[Mg]}{\partial T}\right)dT + \left(\frac{\partial[Mg]}{\partial F_{evap}}\right)dF_{evap} + \left(\frac{\partial[Mg]}{\partial F_{input}}\right)dF_{input} \quad (3)$$

where $\delta^{18}O$ is the oxygen isotopic composition of the lake water determined from biogenic carbonate measurements corrected for species-specific vital effects, [Mg] and [Sr] are the lake water concentrations of Mg^{2+} and Sr^{2+} determined from the Sr/Ca and Mg/Ca ratios measured in the biogenic carbonate, T is mean annual surface air temperature (K) for the lake basin, F_{evap} is the fraction of the lake evaporation, and F_{input} is the fractional lake volume increase due to changes in runoff and precipitation (see table 1).

We treat equations 1-3 as a system of total differential equations that can be solved for each time step of the first derivative of the [Mg], [Sr], and $\delta^{18}O$ time series (that is, $x = \mathbf{A}^{-1}b$, where matrix **A** is composed of the partial derivatives, the b vector is the first derivative of the input dataset (left side of eqs 1 to 3) and x is the solution vector of (dT, dF_{evap}, and dF_{input})). We do so by determining the partial derivatives for a specific lake system, calibrated using modern watershed/lake chemistry data and knowledge of the specific ostracod species. Interpolation to an evenly spaced time series is required, which we accomplish using an Epanechnikov kernel smoother applied to the input data. We assume that within each time step, lake evaporation and/or lake volume change does not change more than 20%, and we approximate all derivatives according to this assumption (that is at 10%). The model output is a time series of the solution

vector (dT, dF_{evap}, and dF_{input}). dF_{evap} and dF_{input} are combined to give the fractional net volume increase for each time-step (see fig. A1). We use a Monte Carlo approach to account for uncertainty in the input parameters and in the input dataset, which we derive from kernel smoothing.

Monte Carlo routine for uncertainty quantification

Given the assumptions that underlie the input parameters and data set for this model it is critical to quantitatively assess the errors associated with the calculated runoff input, temperature changes, and evaporative effects. Thus, we use a Monte Carlo routine to account for two types of uncertainty. The first is uncertainty in the input dataset. Since most paleoclimate records display uneven variance and non-uniform sampling density, it is necessary to account for this by producing datasets for each iteration based on the statistics (time series of the mean and residuals) derived from kernel smoothing of the dataset (see below). To do so, for each Monte Carlo iteration we implement a bootstrapping method whereby we account for input dataset uncertainty by re-sampling residuals. The second type of uncertainty accounted for by our model is the uncertainty in the input parameters. The input parameters are best determined by modern watershed and lake chemistry (when available) and knowledge of the species precipitating the biogenic carbonate (described below). Within each Monte Carlo iteration, we derive a time series of partial derivatives based on the input parameters. Input parameter uncertainty distributions are assumed to be normal distributions, requiring that uncertainty is quantified by as many modern measurements of watershed chemistry as possible. The partial derivatives are substituted into the **A** matrix at each time step.

193 *Input dataset requirements and interpolation*

194 There are two requirements for the input dataset that need to be met for this model. First,
195 the modeled Mg/Ca, Sr/Ca, and $\delta^{18}O$ time series must be of sufficient resolution to resolve
196 climatic events of interest and the time step must be greater than the residence time of these
197 elements in a lake. Thus, in order to use the dataset in the system of equations (left side of eqs 1
198 to 3), the time series must be interpolated to even time steps, requiring a sufficiently resolved age
199 model for the Mg/Ca, Sr/Ca, and $\delta^{18}O$ measurements. Smoothing of each time series (Mg/Ca,
200 Sr/Ca, and $\delta^{18}O$) is performed using an Epanechnikov kernel and interpolated to an even time
201 step following a data driven least squares cross-validation to select the appropriate kernel
202 bandwidth (Hayfield and Racine, 2008). The Epanechnikov kernel (Epanechnikov, 1969) is used
203 because it has finite boundaries (instead of Gaussian kernel) and is smooth (compared to a
204 triangle or uniform kernel) (see Fan, 1992; Danese and others, 2014). Kernel smoothing of the
205 time series is implemented using the 'np' package in R (Hayfield and Racine, 2008). The
206 additional advantage of using a kernel smoother is that uncertainty of the interpolated dataset can
207 be quantified along the time series (mean and residuals) and input into the Monte Carlo routine.

208 While high-resolution interpolation of the smoothed dataset is desirable to resolve
209 climatic events of interest, linear interpolation of the input dataset to an even time step (Δt) must
210 be such that $\Delta t >> \tau_{res}$, where τ_{res} is the residence time (inferred from lake geometry and average
211 input or evaporative fluxes, for example Gibson and others, 2002; Jasechko and others, 2014).
212 For lakes with no modern analogue (see Cretaceous Songliao Basin example), first-order
213 estimates for τ_{res} can be approximated using scaling relationships between outcrop size and basin
214 geometry (Hendriks and others, 2012), which in combination with facies identification can be
215 used to determine estimates of the relationship between potential accommodation and basin

216 average precipitation/evaporation (Carroll and Bohacs, 1999). Thus, due to the formulation and
217 assumptions of the mixing and mass conservation relationships derived below, resolving
218 hydrologic or climatic events over intervals equal to or shorter than τ_{res} is not possible within this
219 modeling framework. This implies that, given the 'water equivalency rule' for a region of
220 interest (Hendriks and others, 2012), paleoclimate records from small lake systems, which
221 integrate smaller watersheds and have shorter residence times, provide the highest fidelity
222 temporal records of hydrologic cycle changes. Furthermore, determination of the lake
223 hypsometry and/or outcrop extent (for example, Reheis 1999; Sack, 2009; Steinman and others,
224 2013; Smith and others, 2014; Doebbert and others, 2014) ensures that the modeling assumptions
225 outlined above are met.

226 The second requirement for the model is that all of the input data need to be placed in
227 terms of lake composition. Although we use measured values of Mg/Ca, Sr/Ca, and $\delta^{18}O$ of
228 ostracods, these values need to be corrected so that they represent the values of these elements
229 and isotopes in the lake water. To make this correction one must correct for "vital effects" and
230 temperature. Correcting for vital effects is relatively straightforward as the measured vital effect
231 is simply subtracted from the measured ostracod values. Vital effects associated with the
232 calcification of biogenic carbonate are observed because shell carbonate is not precipitated in
233 isotopic equilibrium with water (Holmes and Chives, 2002). Vital effects observed in ostracod
234 $\delta^{18}O$ are positive (0.3 to 2.5 ‰) and have been observed to be constant within individual genera
235 (Xia and others, 1997a,b; von Grafenstein and others, 1999; Chivas and others, 2002; Didie and
236 Bauch, 2002). Since vital effects are not temperature-dependent, data from a variety of different
237 modern species fall on slopes close to the inorganic calcite equilibrium slope (-0.250 ‰/K) of
238 Kim and O'Neill (1997) (see compilation by Marco-Barab and others, 2012). Our model ideally

should be used with a time series produced by a single ostracod species or genera. Although, if multiple species are measured (for example, Lister and others, 1991) this could be accounted for using vital effect offsets.

In contrast, correcting for temperature effects is less straightforward and could, if done incorrectly, lead to "circular reasoning" since we are attempting to constrain temperature changes in the model. We assume temperature could vary from 10 to 35 °C (uniform distribution). For each Monte Carlo iteration we select a starting temperature and assume that $\delta^{18}O$ of the lake water is in equilibrium with the measured $\delta^{18}O$ of ostracods using the temperature-dependent fractionation relationship of Kim and O'Neill (1997) corrected for vital effects. We avoid "circular reasoning" since our system of linear equations calculates the relative changes in temperature, dT (in the x vector), using the first derivative of the $\delta^{18}O$ of the lake water (in the b vector), not the absolute temperature.

Distribution coefficients (K_D-values) relating trace element to calcium ratios are commonly determined for biogenic carbonates through modern and/or culturing studies. The distribution (or partition) coefficient is defined as:

$$K_D[M] = \frac{M/Ca_{water}}{M/Ca_{shell}} \quad (4)$$

where M is the trace metal, such as Sr, Mg, or U, and M/Ca are molar ratios. K_D-values for Mg and Sr are both less than one, meaning that both trace metals are actively excluded during calcification. Additionally, Chivas and others (1986b) demonstrated that K_D-values are similar among members of the same or closely related genera.

In many species, K_D has been shown to be temperature-dependent. In most ostracod species, there is little or no temperature effect on Sr/Ca (Chivas and others, 1986; Holmes and Chivas, 2002, Marco-Barab and others, 2012), but the Mg/Ca K_D in ostracods is temperature-

dependent (Engstrom and Nelson, 1991; DeDeckker and others, 1999; Holmes and Chivas, 2002). For the example datasets used in this paper, we use species-specific K_D-values (or from related genera when not available), and uncertainties are obtained from regression statistics of the original datasets (table 2). To place the input data [Mg] and [Sr] in terms of lake composition (b vector) we calculate the Mg/Ca K_D (and Sr/Ca K_D if necessary) using the temperature and lake water [Ca] selected for each Monte Carlo iteration.

Determining Partial Derivatives

In the following sections each of the partial derivatives are derived or determined using either mass conservation (for example, $\frac{\partial[\mathrm{Mg}]}{\partial \mathrm{F}_{\mathrm{evap}}}$) and mixing (for example, $\frac{\partial[\mathrm{Mg}]}{\partial \mathrm{F}_{\mathrm{vol}}}$), or empirical relationships from environmental and/or laboratory measurements (for example, $\frac{\partial\left(\delta^{18}\mathrm{O}\right)}{\partial \mathrm{T}}$).

Temperature Partial Derivatives

To solve for the oxygen isotope partial derivative $\frac{\partial\left(\delta^{18}\mathrm{O}\right)}{\partial \mathrm{T}}$ requires knowing how δ^{18}O of meteoric water (precipitation and runoff) varies as a function of temperature. We recognize that there are numerous factors affecting the δ^{18}O of precipitation beyond that of temperature, which include seasonality, vapor recycling, moisture source et cetera. However, the commonly held assumption that underpins terrestrial paleoclimate studies is the well-known positive correlation between δ^{18}O values of precipitation and temperature for temperate and high latitude areas (Dansgaard, 1964). For the mid-latitude site (Songliao Basin) we use the observed relationship between temperature and precipitation Rozanksi and others (1993) of 0.58 ‰/K, as has been used in numerous studies to calculate the temperature for paleoclimate archives in mid- to high-

latitude sites, such as paleosols (for example, Koch and others, 2003), paleolakes (for example, Anderson and others, 2001), and ice cores (see Jouzel and others, 1997 and references therein). For the low latitude site (Lake Miragoane, Haiti) it is unlikely that the correlations of Rozanksi and others (1993) apply as these are for mid- to high-latitudes. Although it is not ideal to use the approach we outline in this paper to low latitudes because temperature is not as well correlated to the δ^{18}O of precipitation, we use this site only as an example of how this approach can be used in lakes because this record offers the type of data that are necessary for these calculations. Recognizing these limitations we use a slope of 0.26‰/K for the tropical sites (see fig. A2). For both cases we incorporate the error associated with the empirical temperature vs. δ^{18}O correlation in the Monte Carlo.

In our model, thus, one of the assumptions inherent in our calculations is that temperature is the primary driver of δ^{18}O value of water input to the lake. Note that since the slope between temperature and δ^{18}O of precipitation can and does vary geographically, more accurate approaches can the tailored for individual sites by measurements of site-specific correlations between temperature and δ^{18}O of precipitation.

In addition, to the partial $\frac{\partial\left(\delta^{18}\mathrm{O}\right)}{\partial \mathrm{T}}$ discussed above it is necessary to place the ostracod values as the δ^{18}O of lake water for these calculations (b vector of eqs 1 to 3). To do this we need to account for both vital effects and the temperature-dependent isotopic fractionation (see above).

In addition, there are minor temperature effects on the Sr/Ca (typically none) and Mg/Ca (see above discussion). Since the inputs (b vector of eqs 1 to 3) are placed in terms of lake composition, after accounting for the Mg/Ca or Sr/Ca of the lake water and selected temperature

for the Monte Carlo iteration the temperature partial derivatives ($\frac{\partial[\mathrm{Mg}]}{\partial \mathrm{T}}$ and $\frac{\partial[\mathrm{Sr}]}{\partial \mathrm{T}}$) are equal to zero.

Evaporation Partial Derivatives

To account for the evaporative concentration of trace elements, we assume mass conservation of Sr and Mg. Thus, this model is not applicable to brine or saline environments (see Jones and others, 1977; Eugster and Jones, 1979) nor is it applicable to systems that form large deposits of chemical sediments with high Mg and/or Sr concentrations. For biogenic carbonates, we apply the applicable distribution coefficient (K_D) and take the first derivative. In doing so, we assume that the Sr/Ca and Mg/Ca measured in the biogenic carbonates are faithfully recording changes in the Sr and Mg concentrations of the lake water. Assuming mass conservation, the change in solute M concentration (from the initial concentration to an increased concentration at time 2) during fractional lake evaporation (F_{evap}, fraction remaining, from 0 to 1, where 1 is fully evaporated) is given by the equation (fig. 1):

$$[\mathrm{M}]_2 = \frac{[\mathrm{M}]_{\mathrm{initial}}}{(1 - \mathrm{F}_{\mathrm{evap}})} \tag{5}$$

Solving for the partial derivative of equation 5 has the analytical solution:

$$\frac{\partial[\mathrm{M}]}{\partial \mathrm{F}_{\mathrm{evap}}} = \frac{[\mathrm{M}]_{\mathrm{initial}}}{(1 - \mathrm{F}_{\mathrm{evap}})^2} \tag{6}$$

This relationship is non-linear; thus, to provide a linear slope for $\frac{\partial[\mathrm{M}]}{\partial \mathrm{F}_{\mathrm{evap}}}$ we assume that for any given time step, the lake does not evaporate more than 20% by volume. By inspection of equation 6, the average evaporation between 0 to 20%, given by $\mathrm{F}_{\mathrm{evap}} = 0.1$, yields a slope of

$\frac{[M]_{initial}}{(0.9)^2}$. Therefore, the initial trace element concentration (that is, the Mg and Sr concentrations), which we assume to be approximated using the observed distribution of trace element measurements, is important for setting $[M]_{initial}$ at each time step.

The evaporative enrichment of lake water $\delta^{18}O$ with progressive evaporation was originally parameterized by Craig and Gordon (1965). The limitation of applying the Craig and Gordon (1965) evaporation model to lacustrine paleoclimate records, as outlined in detail by Gonfiantini (1986), is the large number of input parameters and the difficulty in constraining the isotopic composition of the evaporated water vapor (see discussion in Jones and Imbers, 2010). Recent work has attempted to simplify evaporative assumptions (Benson and White, 1994; Jones and others, 2007; Jones and Imbers, 2010; Placzek and others, 2011), but numerous input parameters are still required, making the generic application of these lake water evaporation models to paleoclimate records challenging.

Central to the difficulties encountered by previous researchers is the influence of humidity on the evolution of the isotopic composition of an evaporating water body (Gonfiantini, 1986). This is due to changes in the kinetic enrichment factor due to changes in humidity (Gat, 1970; Merlivat, 1978; Merlivat and Jouzel, 1979). However, if within a given time step lake evaporation does not exceed ~25% total lake volume and humidity is <90%, the isotopic evolution of an evaporating water body can be approximated by a Rayleigh relationship (Gonfiantini, 1986). Thus, we derive the partial derivative for $\delta^{18}O$ and fractional lake evaporation as the first derivative of the Rayleigh equation (fig. 1):

$$\frac{\partial(\delta^{18}O)}{\partial F_{evap}} = (\alpha - 1)(\delta^{18}O_1 + 1000)(1 - F_{evap})^{(\alpha-2)} \quad (7)$$

where α is the combined fractionation factor of the temperature-dependent equilibrium fractionation factor (Horita and Weslowski, 1996) and humidity-dependent kinetic fractionation factor (Gonfiantini, 1986), F_{evap} is the fraction of the lake evaporation (as above) and $\delta^{18}O_{initial}$ is the initial isotopic composition of the lake from the measured $\delta^{18}O$ of the biogenic carbonate corrected for vital effects (see below). While a simplification of evaporative processes, assuming a Rayleigh relationship and a combined fractionation factor in this manner has successfully been applied to both surface soil reservoir and lake system modeling (for example, Chamberlain and others, 2014; Caves and others, 2015). We assume that relative humidity for each Monte Carlo iteration can vary from 50 to 90 % (uniform distribution), and temperature varies from 5 to 35 °C (uniform distribution) as determined for each iteration (as described above). By doing so we calculate the combined fractionation factor, α, using the equations of Horita and Weslowski (1996) and Gonfiantini (1986) (see fig. 1). The humidity and temperature ranges selected here are conservative and broadly apply to both illustrative lake systems used in the examples below. The relevant latitude and geographic setting of the lake system being modeled should inform the humidity and temperature ranges chosen as model input.

Lake Input Partial Derivatives

Determination of the lake input partial derivatives is similar for both trace elements and oxygen isotopes. We rely on binary mixing equations assuming that the isotopic and chemical composition of water entering the lake is sufficiently well characterized and relatively invariant (relative to the lake water). Water in terminal lakes is sufficiently evaporatively enriched relative to the input $\delta^{18}O$ that in most examples, the input water $\delta^{18}O$ composition is typically statistically distinguishable from the lake water $\delta^{18}O$ composition (see for example compilation by Horton

368 and Oze, 2012). This is similar for trace elements in terminal lake systems, such that the input
369 concentration of Sr and Mg in terminal lakes is typically more dilute than the lake water.

370 Given these principles, we define the partial derivative relating increased lake volume,
371 from the addition of source water (F_{input}, which varies from 1 to infinity, where 1 is the original
372 lake volume) and variations in $\delta^{18}O$ as the first derivative of a binary mixing relationship (fig. 2):

373 $$\frac{\partial(\delta^{18}O)}{\partial F_{input}} = \frac{(\delta^{18}O)_{source} - (\delta^{18}O)_{initial}}{(F_{evap})^2} \quad (8)$$

374 where $\delta^{18}O_{source}$ is the meteoric water composition and $\delta^{18}O_{initial}$ is determined as previously
375 described. The meteoric water $\delta^{18}O$ composition should be determined by direct observation, by
376 upstream fluvial carbonates (for example Ibarra and others, 2015) or by assuming an empirical
377 relationship related to the amount of annual rainfall (amount effect), as observed in many
378 tropical systems (Risi and others, 2008). Similarly for trace element concentrations:

379 $$\frac{\partial[M]}{\partial F_{input}} = \frac{[M]_{source} - [M]_{initial}}{(F_{evap})^2} \quad (9)$$

380 where M is the Sr or Mg concentration, $[M]_{source}$ refers to the runoff water concentrations, and
381 $[M]_{initial}$ is determined as previously described from the measured Mg/Ca and Sr/Ca of the
382 biogenic carbonate.
383
384 *Input parameter requirements*

385 There are several input parameter requirements that need to be satisfied for robust use of
386 this model. First, measurements of solute chemistry ([Sr], [Mg], and [Ca] from lake water and/or
387 runoff) and $\delta^{18}O$ of meteoric water are necessary to constrain the mixing equation end-members.
388 This can best be done by measuring the elemental and isotopic composition of modern rivers and
389 precipitation in the lake to be studied or the site of the ancient lake as is done here in the

Songliao Basin (table 2). There are obvious complications to this approach since the drainage basin may have changed through time as well as the isotopic composition of precipitation – for example by a change in moisture source. In addition, the uncertainty (standard deviation) of the end-members is required. This can be quantified through repeat measurements of stream water/subsurface runoff chemistry.

Second, empirical relationships for temperature effects on the species-specific partition coefficient (for Mg/Ca) are required; such as those fit by Engstrom and Nelson (1991) and DeDeckker and others (1999). As discussed above, species-specific vital effects for $\delta^{18}O$ offsets are applied uniformly prior to derivation of the partial derivatives from the mixing and mass conservation equations. Input parameters are supplied to HyBIM as the mean and standard deviation, assuming a normal distribution. However, implementation of other probability distributions (such as uniform distributions) is possible. The probable temperature and relative humidity ranges (used for the $\delta^{18}O$ equilibrium fractionation equations and Mg/Ca K_D values), which are treated as uniform distributions, are specified by the user and should be informed by paleoenvironmental, latitudinal, climate modeling, and/or modern observations.

EXAMPLE APPLICATIONS

We apply HyBIM to two lacustrine paleoclimate records covering differing timescales, geochemical conditions, ostracod species, and dataset resolutions (figs. 3 and 4). We chose these two data sets because: (1) they had the elemental and isotopic measurements necessary for using this model and; (2) they represent two very different cases that demonstrate the utility and flexibility and limitations of the HyBIM for a variety of biogenic carbonate paleoclimate records. In each case, the original age model is used for all datasets and input parameters are constrained

using modern catchment and lake chemistry and species-specific partition coefficient calibrations. Sampling resolution, the least squares cross-validated kernel bandwidths, length of the paleoclimate record, and input parameter sources are listed in table 2.

Lake Miragoane, Haiti (Hodell and others, 1991; Curtis and Hodell, 1993)

The paleoclimate records from Holocene Lake Miragoane in Haiti (Hodell and others, 1991; Curtis and Hodell, 1993; Higuera-Gundy, 1999) were one of the first to use detailed, high-resolution stable isotope and trace element measurements on lacustrine ostracods. This hydrologically closed lake provides a complete record of the Holocene at high resolution (see age resolutions for $\delta^{18}O$, Mg/Ca and Sr/Ca records in table 2). Two cores were recovered and sampled at fine (~10 cm) resolution for $\delta^{18}O$ and coarser (~150 cm) resolution for Mg/Ca and Sr/Ca (Curtis and Hodell, 1993). The discrepancy in sample resolution results in the cross-validated kernel bandwidth for $\delta^{18}O$ (bandwidth = 39 years) to be much shorter than the Mg/Ca and Sr/Ca records (422 and 440 years, respectively) (fig. 3A). Data from both cores were combined and kernel smoothed using the original age model.

The elemental and isotopic data for these studies were from ostracods identified as *Candona* sp., by R. Forester (see discussion in Curtis and Hodell, 1993), which is an ostracod species closely related to *Candona rawsoni*. See table 2 for detailed model input parameters, including the partition coefficients for *Candona rawsoni* as determined by Engstrom and Nelson (1991).

The modeled temperature and lake volume changes for the Lake Miragoane record are largely in accordance with the expected response (see interpretation in Curtis and Hodell, 1993, their fig. 8). These authors suggested based on the isotopic and elemental data that lake levels

436 were highest and climate was “mesic” (wetter and hotter) during the early Holocene, peaking
437 between 7,000 and 4,000 years BP (Hodell and others,1991; Curtis and Hodell, 1993). In the late
438 Holocene they suggest that between ~4,000 and ~2,500 years BP there was a two-step increase in
439 aridity towards lower lake level and increased salinity, based primarily on the oxygen isotopes
440 (Hodell and others, 1991), followed by wetter conditions beginning at ~1,000 year BP based on
441 additional evidence from the trace element measurements (Curtis and Hodell, 1993).
442 Our model agrees with this interpretation and shows that modeled temperature and lake
443 volume covary. Lake volume and temperature increase to a peak at ~6300 years BP, decline to a
444 minimum at ~2000 years BP, and increase again nearing present day. The deglacial warming
445 (~10,000 to 7,000 years BP), and increasing aridity (from ~4,000 to 1,000 years BP) are captured
446 by the predicted temperature fluctuations. Driven by the covariation in the input datasets, the
447 modeled temperature is substantially different than that expected from just using the $\frac{\partial\left(\delta^{18}\mathrm{O}\right)}{\partial \mathrm{T}}$
448 empirical relationship of 0.26 ‰/°C (red line of fig. 3B; relationship derived in fig. A2). In
449 addition, while the higher resolution δ^{18}O record determines the sub-1000-year variations in
450 temperature, the long-term trends largely reflect the trace element records. The sampling
451 resolution discrepancy of the trace elements (low resolution) and δ^{18}O records (high resolution)
452 is not necessarily ideal, but our results demonstrate that, by kernel smoothing the records and
453 interpolating to even time-steps, the problem of differing sampling resolution can be resolved.
454
455 *Songliao Basin, China (Chamberlain and others, 2013)*
456 The Songliao Basin is a Cretaceous terrestrial lake basin that contains up to 10,000 m of
457 fluvial-lacustrine, volcaniclastic and alluvial sediments (Feng and others, 2010; Wang and others,
458 2013). During the first phase (SK-1) of the International Continental Scientific Drilling Project’s

(ICDP) efforts to recover strata covering the entire Cretaceous, a total of 2,486 m of core were recovered that span the late Turonian to the end Cretaceous (Wan and others, 2013; Deng and others, 2013; Wu and others, 2014). Recent paleoclimate reconstruction efforts have used a variety of proxies, including ostracods from lacustrine facies (Chamberlain and others, 2013) and paleosol carbonate nodules (Huang and others, 2013; Gao and others, 2015). We model the Sr/Ca, Mg/Ca and $\delta^{18}O$ ostracod record originally published by Chamberlain and others (2013) spanning 84-88 Ma (fig. 4A). Data is kernel smoothed on the original age model (Wan and others, 2013; Wang and others, 2013; Chamberlain and others, 2013), and this portion of the record was selected because of the high density sampling through this period, relatively stable source area (based on $^{87}Sr/^{86}Sr$), and the likely existence of Ocean Anoxic Event 3 (OAE 3 at ~85.5 Ma; Wagreich, 2012). Because the ostracod genus *Cypridea* sampled by Chamberlain and others (2013) is extinct, we use partition coefficient and vital effect calibrations for the extant genus *Cyprideis*, a closely related genus also of the *Cyprididae* family (table 2). See table 2 for detailed model input parameters.

The relatively invariant (kernel smoothed) Mg/Ca and Sr/Ca records (fig. 4A) result in several interesting observations when HyBIM is applied to the Songliao Basin ostracod record. The Mg/Ca and Sr/Ca records demonstrate much greater spread around the mean kernel-smoothed values and, due to slightly lower sampling density, have a greater cross-validated kernel bandwidth than the $\delta^{18}O$ record (62 kyrs vs. 241 kyrs and 219 kyrs; fig. 4A). Because of the relatively invariant Mg/Ca and Sr/Ca record, the modeled temperature is similar to the result expected if a $\frac{\partial(\delta^{18}O)}{\partial T}$ empirical relationship of 0.58 ‰/°C is applied to the kernel smoothed mean of the $\delta^{18}O$ record (red line in fig. 4B), unlike the Lake Miragoane record.

We applied the HyBIM to a portion of the Songliao record given in Chamberlain and others (2013) from 88 to 84 Ma because this time interval captures a portion of the Oceanic Anoxic Event 3 (OAE 3) during a time of global warming. Moreover, we have excellent oxygen and trace element data for this time range in the Songliao Basin. It is recognized that unlike earlier OAEs, OAE 3, may be a series of events distributed over longer time frames and is recorded predominantly in the western hemisphere (Wagreich, 2012). Thus, we are interested in how the temperature record in the Songlia Basin recorded this "event". Our results show peaks of warming of ~6°C between 86 and 85 Ma and again between 85 and 84 Ma. These two warm periods are consistent with multiple events defining OAE 3, but cannot not be correlated with those in marine sections because: 1) the age constraints in the Songlia Basin lack the necessary time resolution; and 2) there are multiple carbon isotope excursions during OAE 3 that vary both temporally and spatially across the globe (Wagreich, 2012). Nevertheless, our results do show multiple warming events during this time interval of OAE 3. In addition, the HyBIM results agree with the interpretation of increasing lake size, based on outcrop extent, during this time interval (Feng and others, 2010), suggesting that over this interval lake volume increased by ~10%. However, we point out that due to the large spread in the measured Sr/Ca and Mg/Ca, the modeled volume changes are not particularly robust.

LIMITATIONS AND GUIDELINES

The modeling framework presented in this paper represents a new approach to quantitatively constraining the hydrologic balance and temperature fluctuations as recorded by the trace elements and stable isotopes of biogenic lacustrine carbonate. Inherently the modeling

of paleoclimate records requires simplifying assumptions. As such, we provide several guidelines for assessing the potential application of HyBIM to a lake system:

(1) Lake systems with highly variable (inorganic) chemical sedimentation, typically driven by order of magnitude changes in lake level, cannot be modeled using HyBIM. A fundamental assumption of the evaporation partial derivatives is that we assume mass conservation of the trace elements within each time step. In addition, we assume that within each time step lake volume does not change by more than 10% (see derivation of partial derivatives). Thus, HyBIM solutions should be limited to "balanced-filled" (Caroll and Bohacs, 1999) lake systems with biogenic carbonate from periods of similar lithologic deposition.

(2) Many large lakes break up into smaller lakes during desiccation due to complex hypsometric basin geometries and watersheds (for example Quaternary Lake Lahontan; Reheis and others, 2014). While this is not readily assessed from sediment cores alone, we emphasize the need for determination of the lake hypsometry via shoreline and/or outcrop extent (for example, Reheis, 1999; Sack, 2009; Zimmerman and others, 2011; Steinman and others, 2013; Ibarra and others, 2014; Smith and others, 2014; Doebbert and others, 2014). HyBIM should not be applied to these systems over intervals of breakup, as the river chemistry of the smaller lake basins within a large system may differ due to bedrock heterogeneity and catchment weathering processes.

(3) Well-constrained partition coefficients are necessary to place the measured Mg/Ca and Sr/Ca (or other trace element measurements) in terms of lake water concentrations. Presently modern studies of terrestrial biogenic carbonates from ostracods (for example, Engstrom and Nelson, 1991; Xia and others, 1997a,b; Wansard and others, 1998; De

Deckker and others, 1999; Dettman and others, 2002; Holmes and Chivas, 2002; Dwyer and others, 2002; Ito and Forester, 2009; Gouramanis and De Deckker, 2010; Marco-Barba and others, 2012; Börner and others, 2013) represent some of the only calibrated partition coefficients available for use in the HyBIM modeling framework outlined here. Future application of this modeling framework to inorganic carbonate or other types of biogenic carbonate from lake systems will require further measurement of trace elements and calibration of partition coefficients.

(4) We assume that lake water temperature and the basin average air temperature are directly proportional. HyBIM solves for temperature changes (ΔT), not absolute values of temperature, but selects an absolute temperature for each Monte Carlo iteration used for placing the measured Mg/Ca and $\delta^{18}O$ into lake water composition (see previous discussion). For the lake systems with mean annual air temperature greater than 0 °C included in a recent global lake temperature compilation the slope between the mean annual water temperature and mean annual surface air temperature is indistinguishable from 1 (slope = 1.02 ± 0.03 (1σ), $r^2 = 0.94$, n = 81, mean annual air temperatures from 0 to 27 °C; see dataset from Appendix A of Hren and Sheldon, 2012), suggesting that this assumption of proportionality is valid.

CONCLUSIONS AND FUTURE MODEL REFINEMENT

In this paper, we develop and apply a new modeling framework using variations in $\delta^{18}O$ and trace elements (Mg and Sr) measured in biogenic lacustrine carbonates for closed basin lacustrine paleoclimate records. By applying this modeling approach to two ostracod records, we demonstrate the utility of HyBIM to quantify paleoenvironmental changes across different

549 timescales. Due to a lack of significant variation in the (kernel smoothed) Mg/Ca and Sr/Ca
550 records from the Songliao Basin, the $\delta^{18}O$ record primarily controls the predicted temperature
551 fluctuations and the volume changes are minimal. Additionally, the Lake Miragoane results
552 demonstrate how the combination of high-resolution and low-resolution datasets are accounted
553 for by HyBIM via kernel smoothing and interpolation to even time steps. Future application of
554 HyBIM to a high-resolution historical record from a small, constrained terminal lake system will
555 provide the best independent validation of this modeling methodology.

556 Two additions could provide further extensions to this modeling approach. First, over-
557 determination of the **A** matrix by adding a fourth equation to the system of equations describing
558 additional trace elements (such as U or Li; for example Holmes and others, 1995), δD (for
559 example Tierney and others, 2008; Feakins and others, 2014; Kirby and others, 2014) or $\delta^{13}C$
560 (controlled by similar processes described in Li and Ku, 1999; Horton and Oze, 2012; Horton
561 and others, 2015) would provide greater control on the partitioning of salinity changes due to
562 evaporation and dilution by volumetric increases. Second, additional isotope systems, such as Sr
563 or Pb isotopes, could be included as a fourth equation (the **A** matrix would be 4x4) and would
564 extend the function of HyBIM to also de-convolve other possible variables, such multiple
565 riverine inputs, rearrangement of the drainage basin, et cetera. For example, assuming different
566 watershed source regions have different Sr or Pb isotope signatures (and also trace element
567 concentrations and/or meteoric water $\delta^{18}O$ inputs), a fourth set of partial derivatives can be
568 derived to define the relationship between two distinct end-members. This approach could be
569 applied to the full Songliao Basin record (lower resolution) presented in Chamberlain and others
570 (2013), or to basins with sufficient data and known tectonic changes, such as Cenozoic basins in

571 the western United States (for example, Davis and others, 2009; Smith and others, 2014;
572 Doebbert and others, 2014).

573 The application of this modeling framework is not limited solely to lake systems. For
574 example, recently published speleothem records have measured $\delta^{18}O$, Mg/Ca, and Sr/Ca, in
575 addition to other trace elements (such as U/Ca, Ba/Ca) and isotope systems (such as ($^{234}U/^{238}U$)
576 and $^{87}Sr/^{86}Sr$) (for example, Oster and others, 2009; Steponaitis and others, 2015). By modifying
577 the modeling framework presented here the relative influence of temperature and vadose zone
578 residence times (influenced by prior carbonate precipitation) on the stable isotope and trace
579 element measurements could be quantitatively deconvolved. However, modern cave monitoring
580 studies to assess the variability and controls on the stable isotope and trace element variations in
581 cave drip water (for example, Fairchild and others, 2000; Musgrove and Banner, 2004; Wong
582 and others, 2011; Oster and others, 2012a), would be necessary for calibration. Similarly, trace
583 element and stable isotope measurements on pedogenic soil minerals and the associated soil pore
584 water in arid soil systems (for example Amundson and others, 1996; Oster and others, 2012b;
585 Maher and others, 2014) may provide an additional avenue for quantitative paleoclimate
586 reconstruction using a similar modeling framework.

587 Finally, the Monte Carlo approach presented in this paper only includes uncertainty in the
588 input parameters and input dataset. However, age-models in sedimentary settings, and many
589 terrestrial paleoclimate archives, including lakes, can be highly uncertain due to sedimentation
590 rate changes, hiatuses and a lack of dateable material (for example, Huybers and Wunsch, 2004;
591 Blaauw and Christen, 2011). Further extension of HyBIM to include incorporation of age model
592 uncertainty would provide added utility by including temporal uncertainty quantification of the
593 hydrologic response to climatic events and trends recorded by the lake carbonate geochemistry.

Recent work has included this type of Monte Carlo age model uncertainty into paleoclimate reconstructions for individual records and large paleoclimate compilations (for example, Shakun and others, 2012; Anchukaitis and Tierney, 2013; Tierney and others, 2013; Marcott and others, 2013; Steinman and others, 2014). Ultimately paleoclimate proxy modeling efforts, such as those illustrated in this paper, are only valuable if the uncertainty of the timing and magnitude of climatic changes is robustly quantified.

ACKNOWLEDGEMENTS

We thank Jay Quade and Byron A. Steinman for thorough and thoughtful reviews. We also thank Yuan Gao and Stephan A. Graham for discussing the Songliao Basin stratigraphy and age model, Kate Maher, Jeremy K. Caves, Sarah C. Lummis, Andreas Mulch and Andrea J. Ritch for thorough discussions and comments, and Bala Rajaratnam for discussing the Monte Carlo and kernel smoothing methods. We would like to thank Sherman Roth-Maher for his insightful comments on the formulation of this model. Daniel E. Ibarra is partially supported by a Stanford EDGE-STEM Fellowship. The Songliao Basin drilling project was supported by the National Basic Research Program of China (2012CB822000) and the China Geological Survey. This research was supported by a National Science Foundation grant (EAR-1423967) to C. Page Chamberlain.

612 REFERENCES

613 Amundson, R., Chadwick, O., Kendall, C., Wang, Y., and DeNiro, M., 1996, Isotopic evidence
614 for shifts in atmospheric circulation patterns during the late Quaternary in mid–North
615 America: Geology, v. 24, no. 1, p. 23–26.
616 Anchukaitis, K.J., and Tierney, J.E., 2012, Identifying coherent spatiotemporal modes in time-
617 uncertain proxy paleoclimate records: Climate dynamics, v. 41, no. 5-6, p. 1291–1306.
618 Anderson, L., Abbott, M.B., and Finney, B.P., 2001, Holocene climate inferred from oxygen
619 isotope ratios in lake sediments, Central Brooks Range, Alaska: Quaternary Research, v.
620 55, no. 3, p. 313–321.
621 Antevs, E.V., 1948, The Great Basin, with emphasis on glacial and postglacial times; climatic
622 changes and pre-white man: Bulletin of the University of Utah, v. 38, p. 168-191.
623 Bengtsson, L., and Malm, J., 1997, Using rainfall-runoff modeling to interpret lake level data:
624 Journal of Paleolimnology, v. 18, no. 3, p. 235–248.
625 Bennett, C.E., Williams, M., Leng, M.J., Siveter, D.J., Davies, S.J., Sloane, H.J., and Wilkinson,
626 I.P., 2011, Diagenesis of fossil ostracods: Implications for stable isotope based
627 palaeoenvironmental reconstruction: Palaeogeography, Palaeoclimatology,
628 Palaeoecology, v. 305, no. 1-4, p. 150–161.
629 Benson, L., and Paillet, F., 2002, HIBAL: A hydrologic-isotopic-balance model for application
630 to paleolake systems: Quaternary Science Reviews, v. 21, no. 12-13, p. 1521–1539.
631 Benson, L.V., and Paillet, F.L., 1989, The use of total lake-surface area as an indicator of
632 climatic change: Examples from the Lahontan basin: Quaternary Research, v. 32, no. 3, p.
633 262–275.
634 Benson, L.V., and White, J.W.C., 1994, Stable isotopes of oxygen and hydrogen in the Truckee

River-Pyramid Lake surface-water system. 3. Source of water vapor overlying Pyramid Lake: Limnology and Oceanography, v. 39, no. 8, p. 1945–1958.

Binford, M.W., Kolata, A.L., Brenner, M., Janusek, J.W., Seddon, M.T., Abbott, M., and Curtis, J.H., 1997, Climate Variation and the Rise and Fall of an Andean Civilization: Quaternary Research, v. 47, no. 2, p. 235–248.

Blaauw, M., and Christen, J.A., 2011, Flexible paleoclimate age-depth models using an autoregressive gamma process: Bayesian Analysis, v. 6, no. 3, p. 457–474.

Blome, M.W., Cohen, A.S., and Lopez, M.J., 2014, Modern distribution of ostracodes and other limnological indicators in southern Lake Malawi: implications for paleocological studies: Hydrobiologia, v. 728, no. 1, p. 179–200.

Bohacs, K.M., Carroll, A.R., and Neal, J.E., 2003, Lessons from large lake systems-thresholds, nonlinearity, and strange attractors, *in* Chan, M.A., and Archer, A.W., editors, Extreme depositional environments: mega end members in geologic time: Geological Society of America Special Paper 370, p. 75-90.

Bowen, G.J., and Revenaugh, J., 2003, Interpolating the isotopic composition of modern meteoric precipitation: Water Resources Research, v. 39, no. 10, p. SWC91–SWC913.

Bowler, J.M., 1981, 30. Australian salt lakes - A palaeohydrologic approach: Hydrobiologia, v. 81-82, no. 1, p. 431–444.

Börner, N., De Baere, B., Yang, Q., Jochum, K.P., Frenzel, P., Andreae, M.O., and Schwalb, A., 2013, Ostracod shell chemistry as proxy for paleoenvironmental change: Quaternary International, v. 313-314, p. 17–37.

Broecker, W., 2010, Long-term water prospects in the Western United States: Journal of Climate, v. 23, no. 24, p. 6669–6683.

658 Burnett, A.W., Kirby, M.E., and Mullins, H.T., 2003, Increasing Great Lake-effect snowfall
659 during the twentieth century: a regional response to global warming?: Journal of Climate,
660 v. 16, no. 21, p. 3535-3542.
661 Carroll, A.R., 1998, Upper Permian lacustrine organic facies evolution, Southern Junggar Basin,
662 NW China: Organic Geochemistry, v. 28, no. 11, p. 649–667.
663 Carroll, A.R., and Bohacs, K.M., 1999, Stratigraphic classification of ancient lakes: Balancing
664 tectonic and climatic controls: Geology, v. 27, no. 2, p. 99–102.
665 Chamberlain, C.P., Wan, X., Graham, S.A., Carroll, A.R., Doebbert, A.C., Sageman, B.B.,
666 Blisniuk, P., Kent-Corson, M.L., Wang, Z., and Chengshan, W., 2013, Stable isotopic
667 evidence for climate and basin evolution of the Late Cretaceous Songliao basin, China:
668 Palaeogeography, Palaeoclimatology, Palaeoecology, v. 385, p. 106–124.
669 Chivas, A.R., De Deckker, P., and Shelley, J.M.G., 1986, Magnesium content of non-marine
670 ostracod shells: A new palaeosalinometer and palaeothermometer: Palaeogeography,
671 Palaeoclimatology, Palaeoecology, v. 54, no. 1-4, p. 43–61.
672 Chivas, A.R., De Deckker, P., Wang, S.X., and Cali, J.A., 2002, Oxygen-Isotope Systematics of
673 the Nektic Ostracod Australocypris Robusta: Geophysical Monograph Series, American
674 Geophysical Union, Washington, D. C., 13 p.
675 Cohen, A., Palacios-Fest, M., Negrini, R., Wigand, P., and Erbes, D., 2000, A paleoclimate
676 record for the past 250,000 years from Summer Lake, Oregon, USA: II. Sedimentology,
677 paleontology and geochemistry: Journal of Paleolimnology, v. 24, no. 2, p. 151–182.
678 Colman, S.M., Peck, J.A., Karabanov, E.B., Carter, S.J., Bradbury, J.P., King, J.W., and
679 Williams, D.F., 1995, Continental climate response to orbital forcing from biogenic silica
680 records in Lake Baikal: Nature, v. 378, p. 769–771.

681 Craig, H., and Gordon, L.I., 1965, Deuterium and oxygen-18 variations in the ocean and the
682 marine atmosphere, *in* Tongiorgi, E., editor, Stable Isotopes in Oceanographic Studies
683 and Paleotemperatures: Pisa, Consiglio Nazionale delle Riche, Laboratorio de Geologia
684 Nucleare, p. 1-122.
685 Currey, D.R., 1990, Quaternary palaeolakes in the evolution of semidesert basins, with special
686 emphasis on Lake Bonneville and the Great Basin, U.S.A: Palaeogeography,
687 Palaeoclimatology, Palaeoecology, v. 76, no. 3-4, p. 189–214.
688 Curtis, J.H., and Hodell, D.A., 1993, An Isotopic and Trace Element Study of Ostracods from
689 Lake Miragoane, Haiti: A 10,500 Year Record of Paleosalinity and Paleotemperature
690 Changes in the Caribbean: American Geophysical Union, 18 p.
691 Danese, M., Masini, N., Biscione, M., and Lasaponara, R., 2014, Predictive modeling for
692 preventive Archaeology: overview and case study: Central European Journal of
693 Geosciences, v. 6, no. 1, p. 42–55.
694 Dansgaard, W., 1964, Stable isotopes in precipitation: Tellus, v. 16, no. 4, p. 436–468.
695 Davis, S.J., Mix, H.T., Wiegand, B.A., Carroll, A.R., and Chamberlain, C.P., 2009, Synorogenic
696 evolution of large-scale drainage patterns: Isotope paleohydrology of sequential
697 Laramide basins: American Journal of Science, v. 309, no. 7, p. 549–602.
698 De Deckker, P., Chivas, A.R., and Shelley, J.M.G., 1999, Uptake of Mg and Sr in the euryhaline
699 ostracod Cyprideis determined from in vitro experiments: Palaeogeography,
700 Palaeoclimatology, Palaeoecology, v. 148, no. 1-3, p. 105–116.
701 Demko, T.M., Nicoll, K., Beer, J.J., Hasiotis, S.T., and Park, L.E., 2005, Mesozoic lakes of the
702 Colorado Plateau: Field Guides, v. 6, p. 329–356.
703 Deng, C.L., He, H.Y., Pan, Y.X., and Zhu, R.X., 2013, Chronology of the terrestrial Upper

704 Cretaceous in the Songliao Basin, northeast Asia: Palaeogeography, Palaeoclimatology,
705 Palaeoecology, v. 385, p. 44–54.
706 Derry, L.A., and France-Lanord, C., 1996, Neogene growth of the sedimentary organic carbon
707 reservoir: Paleoceanography, v. 11, no. 3, p. 267–275.
708 Dettman, D.L., Palacios-Fest, M., and Cohen, A.S., 2002, Comment on G. Wansard and F.
709 Mezquita, The response of ostracode shell chemistry to seasonal change in a
710 Mediterranean freshwater spring environment: Journal of Paleolimnology, v. 27, no. 4, p.
711 487–491.
712 Doebbert, A.C., Carroll, A.R., Mulch, A., Chetel, L.M., and Chamberlain, C.P., 2010,
713 Geomorphic controls on lacustrine isotopic compositions: Evidence from the Laney
714 Member, Green River Formation, Wyoming: Geological Society of America Bulletin, v.
715 122, no. 1-2, p. 236–252.
716 Doebbert, A.C., Johnson, C.M., Carroll, A.R., Beard, B.L., Pietras, J.T., Rhodes Carson, M.,
717 Norsted, B., and Throckmorton, L.A., 2014, Controls on Sr isotopic evolution in
718 lacustrine systems: Eocene Green River formation, Wyoming: Chemical Geology, v. 380,
719 p. 172–189.
720 Edney, P.A., Kershaw, A.P., and De Deckker, P., 1990, A late Pleistocene and Holocene
721 vegetation and environmental record from Lake Wangoom, Western Plains of Victoria,
722 Australia: Palaeogeography, Palaeoclimatology, Palaeoecology, v. 80, no. 3-4, p. 325–
723 343.
724 Epanechnikov, V.A., 1969, Non-Parametric Estimation of a Multivariate Probability Density:
725 Theory of Probability & Its Applications, v. 14, no. 1, p. 153–158.
726 Engstrom, D.R., and Nelson, S.R., 1991, Paleosalinity from trace metals in fossil ostracodes

compared with observational records at Devils Lake, North Dakota, USA: Palaeogeography, Palaeoclimatology, Palaeoecology, v. 83, no. 4, p. 295–312.

Eugster, H.P., and Jones, B.F., 1979, Behavior of major solutes during closed basin- lakes brine evolution.: American Journal of Science, v. 279, no. 6, p. 609–631.

Eugster, H.P., and Kelts, K., 1983, Lacustrine chemical sediments.: Chemical sediments and geomorphology, p. 321–368.

Fan, J., 2012, Design-adaptive Nonparametric Regression: Journal of the American Statistical Association, v. 87, no. 420, p. 998–1004.

Fantle, M.S., 2010, Evaluating the Ca isotope proxy: American Journal of Science, v. 310, no. 3, p. 194–230.

Fairchild, I.J., Borsato, A., Tooth, A.F., Frisia, S., Hawkesworth, C.J., Huang, Y., McDermott, F., and Spiro, B., 2000, Controls on trace element (Sr–Mg) compositions of carbonate cave waters: implications for speleothem climatic records: Chemical Geology, v. 166, no. 3-4, p. 255–269.

Feakins, S.J., Kirby, M.E., Cheetham, M.I., Ibarra, Y., and Zimmerman, S.R.H., 2014, Fluctuation in leaf wax D/H ratio from a southern California lake records significant variability in isotopes in precipitation during the late Holocene: Organic Geochemistry, v. 66, p. 48–59.

Feng, Z.Q., Jia, C.Z, Xie, X.N., Shun, Z., Feng, Z.H. and Cross, T.A. 2010, Tectonostratigraphic units and stratigraphic sequences of the nonmarine Songliao basin, northeast China: Basin Research, v. 22, no. 1, p. 79–95.

Forester, R.M., 1991, Pliocene-climate history of the western United States derived from lacustrine ostracodes: Quaternary Science Reviews, v. 10, no. 2-3, p. 133–146.

François, L.M., and Goddéris, Y., 1998, Isotopic constraints on the Cenozoic evolution of the carbon cycle: Chemical Geology, v. 145, no. 3-4, p. 177–212.

Frogley, M.R., Griffiths, H.I., and Martens, K., 2002, Modern and Fossil Ostracods From Ancient Lakes, *in* Holmes, J.A., and Chivas, A.R., editors. The Ostracoda: applications in Quaternary research: American Geophysical Union, Geophysical Monograph Series, v. 131, p. 167-184.

Gao, Y., Ibarra, D.E., Wang, C., and Caves, J.K., 2015, Mid-latitude terrestrial climate of East Asia linked to global climate in the Late Cretaceous: Geology, v. 43, no. 4, p. 287–290.

Garnett, E.R., Andrews, J.E., Preece, R.C., and Dennis, P.F., 2004, Climatic change recorded by stable isotopes and trace elements in a British Holocene tufa: Journal of Quaternary Science, v. 19, no. 3, p. 251–262.

Gat, J.R., 1970, Environmental isotope balance of Lake Tiberias: Isotope hydrology.

Gat, J.R., and Matsui, E., 1991, Atmospheric water balance in the Amazon basin: An isotopic evapotranspiration model: Journal of Geophysical Research: Solid Earth (1978–2012), v. 96, no. D7, p. 13179–13188.

Gat, J.R., Bowser, C.J., and Kendall, C., 1994, The contribution of evaporation from the Great Lakes to the continental atmosphere: estimate based on stable isotope data: Geophysical Research Letters, v. 21, no. 7, p. 557–560.

Gibson, J.J., and Edwards, T.W.D., 2002, Regional water balance trends and evaporation-transpiration partitioning from a stable isotope survey of lakes in northern Canada: Global Biogeochemical Cycles, v. 16, no. 2, p. 10–1–10–14.

Gibson, J.J., Prepas, E.E., and McEachern, P., 2002, Quantitative comparison of lake throughflow, residency, and catchment runoff using stable isotopes: modeling and results

773 from a regional survey of Boreal lakes: Journal of Hydrology, v. 262, no. 1-4, p. 128–
774 144.
775 Gibson, J.J., Birks, S.J., and Yi, Y., 2015, Stable isotope mass balance of lakes: a contemporary
776 perspective: Quaternary Science Reviews.
777 Goddéris, Y., and François, L.M., 1996, Balancing the Cenozoic carbon and alkalinity cycles:
778 Constraints from isotopic records: Geophysical Research Letters, v. 23, no. 25, p. 3743–
779 3746.
780 Gonfiantini, R., 1986, Environmental isotopes in lake studies: Handbook of environmental
781 isotope geochemistry, v. 2, p. 113–168.
782 Gouramanis, C., Wilkins, D., and De Deckker, P., 2010, 6000 years of environmental changes
783 recorded in Blue Lake, South Australia, based on ostracod ecology and valve chemistry:
784 Palaeogeography, Palaeoclimatology, Palaeoecology, v. 297, no. 1, p. 223–237.
785 Grafenstein, von, U., Erlernkeuser, H., and Trimborn, P., 1999, Oxygen and carbon isotopes in
786 modern fresh-water ostracod valves: assessing vital offsets and autecological effects of
787 interest for palaeoclimate studies: Palaeogeography, Palaeoclimatology, Palaeoecology, v.
788 148, no. 1-3, p. 133–152.
789 Guay, B.E., Eastoe, C.J., Bassett, R., and Long, A., 2004, Identifying sources of groundwater in
790 the lower Colorado River valley, USA, with $\delta^{18}O$, δD, and 3H: implications for river
791 water accounting: Hydrogeology Journal, v. 14, no. 1-2, p. 146–158.
792 Han, Y., and Huh, Y., 2009, A geochemical reconnaissance of the Duman (Tumen) River and the
793 hot springs of Mt. Baekdu (Changbai): Weathering of volcanic rocks in mid-latitude
794 setting: Chemical Geology, v. 264, no. 1-4, p. 162–172.
795 Hayfield, T., and Racine, J.S., 2008, Nonparametric econometrics: The np package: Journal of

statistical software.

Hendriks, A.J., Schipper, A.M., Caduff, M., and Huijbregts, M.A.J., 2012, Size relationships of water inflow into lakes: Empirical regressions suggest geometric scaling: Journal of Hydrology, v. 414-415, p. 482–490.

Hillman, A.L., Yu, J., Abbott, M.B., Cooke, C.A., Bain, D.J., and Steinman, B.A., 2014, Rapid environmental change during dynastic transitions in Yunnan Province, China: Quaternary Science Reviews, v. 98, p. 24–32.

Hodell, D.A., Curtis, J.H., Higuera-Gundy, A., Brenner, M., Jones, G.A., Binford, M.W., and Dorsey, K.T., 1991, Reconstruction of Caribbean climate change over the past 10,500 years: Nature, v. 352, no. 6338, p. 790–793.

Holmes, J.A., Zhang, J., Chen, F., and Qiang, M., 2007a, Paleoclimatic implications of an 850-year oxygen-isotope record from the northern Tibetan Plateau: Geophysical Research Letters, v. 34, no. 23.

Holmes, J., Darbyshire, D., and Heaton, T., 2007b, Palaeohydrological significance of late Quaternary strontium isotope ratios in a tropical lake: Chemical Geology, v. 236, no. 3-4, p. 281–290.

Holmes, J.A., and Chivas, A.R., 2002, Ostracod Shell Chemistry—Overview, *in* Holmes, J.A., and Chivas, A.R., editors. The Ostracoda: applications in Quaternary research: American Geophysical Union, Geophysical Monograph Series, v. 131, p. 185-204.

Holmes, J.A., Street-Peffott, F.A., Ivanovich, M., and Peffott, R.A., 1995a, A late Quaternary palaeolimnological record from Jamaica based on trace-element chemistry of ostracod shells: Chemical Geology, v. 124, no. 1-2, p. 143–160.

Holmes, J.A., Street-Perrott, F.A., Heaton, T.H.E., Darbyshire, D.P.F., Davies, N.C., and Hales,

P.E., 1995b, Chemical and isotopic composition of karstic lakes in Jamaica, West Indies: Hydrobiologia, v. 312, no. 2, p. 121–138.

Horita, J., 1990, Stable isotope paleoclimatology of brine inclusions in halite: Modeling and application to Searles Lake, California: Geochimica et Cosmochimica Acta, v. 54, no. 7, p. 2059–2073.

Horita, J., and Wesolowski, D.J., 1994, Liquid-vapor fractionation of oxygen and hydrogen isotopes of water from the freezing to the critical temperature: Geochimica et Cosmochimica Acta, v. 58, no. 16, p. 3425–3437.

Horne, D.J., Cohen, A., and Martens, K., 2002, Taxonomy, Morphology and Biology of Quaternary and Living Ostracoda, *in* Holmes, J.A., and Chivas, A.R., editors. The Ostracoda: applications in Quaternary research: American Geophysical Union, Geophysical Monograph Series, v. 131, p. 5-36.

Horton, T.W., and Chamberlain, C.P., 2006, Stable isotopic evidence for Neogene surface downdrop in the central Basin and Range Province: Geological Society of America Bulletin, v. 118, no. 3-4, p. 475–490.

Horton, T.W., and Oze, C., 2012, Are two elements better than one? Dual isotope-ratio detrending of evaporative effects on lake carbonate paleoelevation proxies: Geochemistry, Geophysics, Geosystems, v. 13, no. 6.

Horton, T.W., Defliese, W.F., Tripati, A.K., and Oze, C., 2015, Evaporation induced ^{18}O and ^{13}C enrichment in lake systems: A global perspective on hydrologic balance effects: Quaternary Science Reviews.

Hostetler, S.W., and Benson, L.V., 1994, Stable isotopes of oxygen and hydrogen in the Truckee River-Pyramid Lake surface-water system. 2.A predictive model of delta18O and delta2H

842 in pyramid lake: Limnology and Oceanography, v. 39, no. 2, p. 356–364.
843 Hren, M.T., and Sheldon, N.D., 2012, Temporal variations in lake water temperature
844 Paleoenvironmental implications of lake carbonate $\delta^{18}O$ and temperature records: Earth
845 and Planetary Science Letters, v. 337-338, no. C, p. 77–84.
846 Huang, C., Retallack, G.J., Wang, C., and Huang, Q., 2013, Paleoatmospheric pCO_2 fluctuations
847 across the Cretaceous–Tertiary boundary recorded from paleosol carbonates in NE China:
848 Palaeogeography, Palaeoclimatology, Palaeoecology, v. 385, p. 95–105.
849 Huybers, P., and Wunsch, C., 2004, A depth-derived Pleistocene age model: Uncertainty
850 estimates, sedimentation variability, and nonlinear climate change: Paleoceanography, v.
851 19, no. 1, 24 p.
852 Hudson, A.M., and Quade, J., 2013, Long-term east-west asymmetry in monsoon rainfall on the
853 Tibetan Plateau: Geology, v. 41, no. 3, p. 351–354.
854 Hudson, A.M., Quade, J., Huth, T.E., Lei, G., Cheng, H., Edwards, L.R., Olsen, J.W., and Zhang,
855 H., 2015, Lake level reconstruction for 12.8–2.3ka of the Ngangla Ring Tso closed-basin
856 lake system, southwest Tibetan Plateau: Quaternary Research, v. 83, no. 1, p. 66–79.
857 Huth, T., Hudson, A.M., Quade, J., Guoliang, L., and Hucai, Z., 2015, Constraints on
858 paleoclimate from 11.5 to 5.0ka from shoreline dating and hydrologic budget modeling of
859 Baqan Tso, southwestern Tibetan Plateau: Quaternary Research, v. 83, no. 1, p. 80–93.
860 Ibarra, D.E., Egger, A.E., Weaver, K.L., Harris, C.R., and Maher, K., 2014, Rise and fall of late
861 Pleistocene pluvial lakes in response to reduced evaporation and precipitation: Evidence
862 from Lake Surprise, California: Bulletin of the Geological Society of America, v. 126, no.
863 11-12, p. 1387–1415.
864 Ibarra, Y., Corsetti, F.A., Feakins, S.J., Rhodes, E.J., and Kirby, M.E., 2015, Fluvial tufa

865 evidence of Late Pleistocene wet intervals from Santa Barbara, California, U.S.A.:
866 Palaeogeography, Palaeoclimatology, Palaeoecology, v. 422, p. 36–45.
867 Imberger, J., and Ivey, G.N., 1991, On the nature of turbulence in a stratified fluid. Part II:
868 Application to lakes: J. Physical Oceanography, v. 21, no. 5 May, p. 659–680.
869 Jasechko, S., Gibson, J.J., and Edwards, T.W.D., 2014, Stable isotope mass balance of the
870 Laurentian Great Lakes: Journal of Great Lakes Research, v. 40, no. 2, p. 336–346.
871 Jasechko, S., Sharp, Z.D., Gibson, J.J., Birks, S.J., Yi, Y., and Fawcett, P.J., 2013, Terrestrial
872 water fluxes dominated by transpiration: Nature, v. 496, no. 7445, p. 347–350.
873 Jones, B.F., Eugster, H.P., and Rettig, S.L., 1977, Hydrochemistry of the Lake Magadi basin,
874 Kenya: Geochimica et Cosmochimica Acta, v. 41, no. 1, p. 53–72.
875 Jones, M.D., and Imbers, J., 2010, Modeling Mediterranean lake isotope variability: Global and
876 Planetary Change, v. 71, no. 3-4, p. 193–200.
877 Jones, M.D., Roberts, C.N., and Leng, M.J., 2007, Quantifying climatic change through the last
878 glacial-interglacial transition based on lake isotope palaeohydrology from central Turkey:
879 Quaternary Research, v. 67, no. 3, p. 463–473.
880 Jouzel, J., Alley, R.B., Cuffey, K.M., Dansgaard, W., Grootes, P., Hoffmann, G., Johnsen, S.J.,
881 Koster, R.D., Peel, D., Shuman, C.A., Stievenard, M., Stuiver, M., and White, J., 1997,
882 Validity of the temperature reconstruction from water isotopes in ice cores: Journal of
883 Geophysical Research, v. 102, no. C12, p. 26471–26487.
884 Keatings, K.W., 1999, The Basis for Ostracod Shell Chemistry in Palaeoclimate Reconstruction:
885 Ph.D. thesis, Kingston University, London.
886 Kelts, K., 1988, Environments of deposition of lacustrine petroleum source rocks: an
887 introduction: Geological Society, London, Special Publications, v. 40, no. 1, p. 3–26.

888 Kempf, O., Blisniuk, P.M., Wang, S., Fang, X., Wrozyna, C., and Schwalb, A., 2009,
889 Sedimentology, sedimentary petrology, and paleoecology of the monsoon-driven, fluvio-
890 lacustrine Zhada Basin, SW-Tibet: Sedimentary Geology, v. 222, no. 1-2, p. 27–41.
891 Kim, S.T., and O'Neil, J.R., 1997, Equilibrium and nonequilibrium oxygen isotope effects in
892 synthetic carbonates: Geochimica et Cosmochimica Acta, v. 61, no. 16, p. 3461–3475.
893 Kirby, M.E., Feakins, S.J., Hiner, C.A., Fantozzi, J., Zimmerman, S.R.H., Dingemans, T., and
894 Mensing, S.A., 2014, Tropical Pacific forcing of Late-Holocene hydrologic variability in
895 the coastal southwest United States: Quaternary Science Reviews, v. 102, p. 27–38.
896 Koch, P.L., Clyde, W.C., Hepple, R.P., Fogel, M.L., Wing, S.L., and Zachos, J.C., 2003, Carbon
897 and oxygen isotope records from paleosols spanning the Paleocene-Eocene boundary,
898 Bighorn Basin, Wyoming, *in* Wing, S.L., Gingerich, P.D., Schmitz, B., and Thomas, E.,
899 editors, Causes and consequences of globally warm climates in the early Paleogene:
900 Geological Society of America Special Paper 369, p. 49–64.
901 Krabbenhoft, D.P., Anderson, M.P., and Bowser, C.J., 1990a, Estimating groundwater exchange
902 with lakes 2. Calibration of a three- dimensional, solute transport model to a stable
903 isotope plume: Water Resources Research, v. 26, no. 10, p. 2455–2462.
904 Krabbenhoft, D.P., Bowser, C.J., Anderson, M.P., and Valley, J.W., 1990b, Estimating
905 groundwater exchange with lakes 1. The stable isotope mass balance method: Water
906 Resources Research, v. 26, no. 10, p. 2445–2453.
907 Lamb, H., Roberts, N., Leng, M., Barker, P., Benkaddour, A., and van der Kaars, S., 1999, Lake
908 evolution in a semi-arid montane environment: response to catchment change and
909 hydroclimatic variation: Journal of Paleolimnology, v. 21, no. 3, p. 325–343.
910 Li, G., and Elderfield, H., 2013, Evolution of carbon cycle over the past 100 million years:

Geochimica et Cosmochimica Acta, v. 103, p. 11–25.

Li, G., Ji, J., Chen, J., and Kemp, D.B., 2009, Evolution of the Cenozoic carbon cycle: The roles of tectonics and CO_2 fertilization: Global Biogeochemical Cycles, v. 23, no. 1.

Li, H.C., and Ku, T.L., 1997, δ13C–δ18C covariance as a paleohydrological indicator for closed-basin lakes: Palaeogeography, Palaeoclimatology, Palaeoecology, v. 133, no. 1-2, p. 69–80.

Liu, B., Liu, C.-Q., Zhang, G., Zhao, Z.-Q., Li, S.-L., Hu, J., Ding, H., Lang, Y.-C., and Li, X.-D., 2013, Chemical weathering under mid- to cool temperate and monsoon-controlled climate: A study on water geochemistry of the Songhuajiang River system, northeast China: Applied Geochemistry, v. 31, no. C, p. 265–278.

Maher, K., Ibarra, D.E., Oster, J.L., Miller, D.M., Redwine, J.L., Reheis, M.C., and Harden, J.W., 2014, Uranium isotopes in soils as a proxy for past infiltration and precipitation across the western United States: American Journal of Science, v. 314, no. 4, p. 821–857.

Marco-Barba, J., Ito, E., Carbonell, E., and Mesquita-Joanes, F., 2012, Empirical calibration of shell chemistry of Cyprideis torosa (Jones, 1850) (Crustacea: Ostracoda): Geochimica et Cosmochimica Acta, v. 93, p. 143–163.

Marcott, S.A., Shakun, J.D., Clark, P.U., and Mix, A.C., 2013, A reconstruction of regional and global temperature for the past 11,300 years: Science, v. 339, no. 6124, p. 1198–1201.

Lacustrine cave carbonates: Novel archives of paleohydrologic change in the Bonneville Basin (Utah, USA), 2012, Lacustrine cave carbonates: Novel archives of paleohydrologic change in the Bonneville Basin (Utah, USA): v. 351-352, p. 182–194.

Melles, M., Brigham-Grette, J., Minyuk, P.S., Nowaczyk, N.R., Wennrich, V., DeConto, R.M., Anderson, P.M., Andreev, A.A., Coletti, A., Cook, T.L., Haltia-Hovi, E., Kukkonen, M.,

Lozhkin, A.V., Rosén, P., and others, 2012, 2.8 million years of Arctic climate change from Lake El'gygytgyn, NE Russia: Science, v. 337, no. 6092, p. 315–320.

Menking, K.M., Anderson, R.Y., Shafike, N.G., Syed, K.H., and Allen, B.D., 2004, Wetter or colder during the Last Glacial Maximum? Revisiting the pluvial lake question in southwestern North America: Quaternary Research, v. 62, no. 3, p. 280–288.

Merlivat, L., 1978, The dependence of bulk evaporation coefficients on air-water interfacial conditions as determined by the isotopic method: Journal of Geophysical Research, v. 83, no. C6, p. 2977–2980.

Merlivat, L., and Jouzel, J., 1979, Global climatic interpretation of the deuterium-oxygen 18 relationship for precipitation: Journal of Geophysical Research, v. 84, no. C8, p. 5029–5033.

Mifflin, M.D., and Wheat, M.M., 1979, Pluvial Lakes and Estimated Pluvial Climates of Nevada: Nevada Bureau of Mines and Geology Bulletin, v. 94.

Moon, S., Huh, Y., and Zaitsev, A., 2009, Hydrochemistry of the Amur River: Weathering in a Northern Temperate Basin: Aquatic Geochemistry, v. 15, no. 4, p. 497–527.

Munroe, J.S., and Laabs, B.J.C., 2013, Latest Pleistocene history of pluvial Lake Franklin, northeastern Nevada, USA: Geological Society of America Bulletin, v. 125, no. 3-4, p. 322–342.

Müller, G., Irion, G., and Förstner, U., 1972, Formation and diagenesis of inorganic Ca−Mg carbonates in the lacustrine environment: Naturwissenschaften, v. 59, no. 4, p. 158–164.

Musgrove, M., and Banner, J.L., 2004, Controls on the spatial and temporal variability of vadose dripwater geochemistry: Edwards aquifer, central Texas: Geochimica et Cosmochimica Acta, v. 68, no. 5, p. 1007–1020.

957 Nilsson, E., 1931, Quaternary glaciations and pluvial lakes in British East Africa: Geografiska
958 Annaler, v. 13, p. 249–349.
959 Oster, J.L., Montañez, I.P., Sharp, W.D., and Cooper, K.M., 2009, Late Pleistocene California
960 droughts during deglaciation and Arctic warming: Earth and Planetary Science Letters, v.
961 288, no. 3-4, p. 434–443.
962 Oster, J.L., Montañez, I.P., and Kelley, N.P., 2012a, Response of a modern cave system to large
963 seasonal precipitation variability: Geochimica et Cosmochimica Acta, v. 91, p. 92–108.
964 Oster, J.L., Ibarra, D.E., Harris, C.R., and Maher, K., 2012b, Influence of eolian deposition and
965 rainfall amounts on the U-isotopic composition of soil water and soil minerals:
966 Geochimica et Cosmochimica Acta, v. 88, p. 146–166.
967 Oviatt, C.G., and McCoy, W.D., 1992, Early Wisconsin lakes and glaciers in the Great Basin,
968 U.S.A, *in* Clark, P.U., and Lea, P.D., editors, The Last Interglacial-Glacial Transition in
969 North America: Geological Society of America Special Paper 270, p. 279–288.
970 Partridge, T.C., Demenocal, P.B., Lorentz, S.A., Paiker, M.J., and Vogel, J.C., 1997, Orbital
971 forcing of climate over South Africa: A 200,000-year rainfall record from the Pretoria
972 Saltpan: Quaternary Science Reviews, v. 16, no. 10, p. 1125–1133.
973 Placzek, C.J., Quade, J., and Patchett, P.J., 2011, Isotopic tracers of paleohydrologic change in
974 large lakes of the Bolivian Altiplano: Quaternary Research, v. 75, no. 1, p. 231–244.
975 Poulsen, C.J., Pollard, D., and White, T.S., 2007, General circulation model simulation of the
976 $\delta^{18}O$ content of continental precipitation in the middle Cretaceous: A model-proxy
977 comparison: Geology, v. 35, no. 3, p. 199–202.
978 Reheis, M., 1999, Highest pluvial-lake shorelines and Pleistocene climate of the western Great
979 Basin: Quaternary Research, v. 52, no. 2, p. 196–205.

Reheis, M.C., Adams, K.D., Oviatt, C.G., and Bacon, S.N., 2014, Pluvial lakes in the Great Basin of the western United States-a view from the outcrop: Quaternary Science Reviews, v. 97, p. 33–57.

Royer, D.L., Donnadieu, Y., Park, J., Kowalczyk, J., and Goddéris, Y., 2014, Error analysis of CO_2 and O_2 estimates from the long-term geochemical model GEOCARBSULF: American Journal of Science, v. 314, no. 9, p. 1259–1283.

Rozanski, K., Araguás-Arrguás, L., and Gonfiantini, R., 1993, Isotopic patterns in modern global precipita- tion, *in* Swart, P. K., Lohmann, K. C., McKenzie, J., and Savin, S., editors. Climate Change in Continental Isotopic Records: Washington D. C., American Geophysical Union Geophysical Monograph 78, p. 1–36.

Rozanski, K., Johnsen, S.J., Schotterer, U., and Thompson, L.G., 1997, Reconstruction of past climates from stable isotope records of palaeo-precipitation preserved in continental archives: Hydrological Sciences Journal, v. 42, no. 5, p. 725–745.

Russell, J.M., and Johnson, T.C., 2006, The Water Balance and Stable Isotope Hydrology of Lake Edward, Uganda-Congo: Journal of Great Lakes Research, v. 32, no. 1, p. 77–90.

Sack, D., 2009, Evidence for climate change from desert basin palaeolakes: 14 p.

Shakun, J.D., Clark, P.U., He, F., Marcott, S.A., Mix, A.C., Liu, Z., Otto-Bliesner, B., Schmittner, A., and Bard, E., 2012, Global warming preceded by increasing carbon dioxide concentrations during the last deglaciation.: Nature, v. 484, no. 7392, p. 49–54.

Shapley, M.D., Ito, E., and Donovan, J.J., 2005, Authigenic calcium carbonate flux in groundwater-controlled lakes: Implications for lacustrine paleoclimate records: Geochimica et Cosmochimica Acta, v. 69, no. 10, p. 2517–2533.

Smith, M.E., Carroll, A.R., Jicha, B.R., Cassel, E.J., and Scott, J.J., 2014, Paleogeographic

record of Eocene Farallon slab rollback beneath western North America: Geology, v. 42, no. 12, p. 1039–1042.

Snyder, C.T., and Langbein, W.B., 1962, The Pleistocene Lake in Spring Valley, Nevada, and its climatic implications: Journal of Geophysical Research, v. 67, no. 6, p. 2385–2394.

Stansell, N.D., Steinman, B.A., Abbott, M.B., Rubinov, M., and Roman-Lacayo, M., 2013, Lacustrine stable isotope record of precipitation changes in Nicaragua during the Little Ice Age and Medieval Climate Anomaly: Geology, v. 41, no. 2, p. 151–154.

Steinman, B.A., Rosenmeier, M.F., Abbott, M.B., and Bain, D.J., 2010a, The isotopic and hydrologic response of small, closed-basin lakes to climate forcing from predictive models: Application to paleoclimate studies in the upper Columbia River basin: Limnology and Oceanography, v. 55, no. 6, p. 2231–2245.

Steinman, B.A., Rosenmeier, M.F., and Abbott, M.B., 2010b, The isotopic and hydrologic response of small, closed-basin lakes to climate forcing from predictive models: Simulations of stochastic and mean-state precipitation variations: Limnology and Oceanography, v. 55, no. 6, p. 2246–2261.

Steinman, B.A., and Abbott, M.B., 2013, Isotopic and hydrologic responses of small, closed lakes to climate variability: Hydroclimate reconstructions from lake sediment oxygen isotope records and mass balance models: Geochimica et Cosmochimica Acta, v. 105, p. 342–359.

Steinman, B.A., Abbott, M.B., Mann, M.E., Stansell, N.D., and Finney, B.P., 2012, 1,500 year quantitative reconstruction of winter precipitation in the Pacific Northwest, *in* National Acad Sciences, p. 11619–11623.

Steinman, B.A., Abbott, M.B., Nelson, D.B., Stansell, N.D., Finney, B.P., Bain, D.J., and

1026 Rosenmeier, M.F., 2013, Isotopic and hydrologic responses of small, closed lakes to
1027 climate variability: Comparison of measured and modeled lake level and sediment core
1028 oxygen isotope records: Geochimica et Cosmochimica Acta, v. 105, p. 455–471.
1029 Steinman, B.A., Abbott, M.B., Mann, M.E., Ortiz, J.D., Feng, S., Pompeani, D.P., Stansell, N.D.,
1030 Anderson, L., Finney, B.P., and Bird, B.W., 2014, Ocean-atmosphere forcing of
1031 centennial hydroclimate variability in the Pacific Northwest: Geophysical Research
1032 Letters, v. 41, no. 7, p. 2553–2560.
1033 Steponaitis, E., Andrews, A., McGee, D., Quade, J., Hsieh, Y.-T., Broecker, W.S., Shuman,
1034 B.N., Burns, S.J., and Cheng, H., 2015, Mid-Holocene drying of the U.S. Great Basin
1035 recorded in Nevada speleothems: Quaternary Science Reviews.
1036 Talbot, M.R., 1990, A review of the palaeohydrological interpretation of carbon and oxygen
1037 isotopic ratios in primary lacustrine carbonates: Chemical Geology: Isotope Geoscience
1038 Section, v. 80, no. 4, p. 261–279.
1039 Tierney, J.E., Russell, J.M., Huang, Y., Damsté, J.S.S., Hopmans, E.C., and Cohen, A.S., 2008,
1040 Northern hemisphere controls on tropical southeast African climate during the past
1041 60,000 years: Science, v. 322, no. 5899, p. 252–255.
1042 Tierney, J.E., Smerdon, J.E., Anchukaitis, K.J., and Seager, R., 2013, Multidecadal variability in
1043 East African hydroclimate controlled by the Indian Ocean.: Nature, v. 493, no. 7432, p.
1044 389–392.
1045 Wagreich, M., 2012, “OAE 3” - Regional Atlantic organic carbon burial during the Coniacian-
1046 Santonian: Climate of the Past, v. 8, no. 5, p. 1447–1455.
1047 Wan, X., Zhao, J., Scott, R.W., Wang, P., Feng, Z., Huang, Q., and Xi, D., 2013, Late
1048 Cretaceous stratigraphy, Songliao Basin, NE China: SK1 cores: Palaeogeography,

1049 Palaeoclimatology, Palaeoecology, v. 385, p. 31–43.
1050 Wang, B., Lee, X.-Q., Yuan, H.-L., Zhou, H., Cheng, H.-G., Cheng, J.-Z., Zhou, Z.-H., Xing, Y.,
1051 Bin Fang, Zhang, L.-K., and Yang, F., 2012, Distinct patterns of chemical weathering in
1052 the drainage basins of the Huanghe and Xijiang River, China: Evidence from chemical
1053 and Sr-isotopic compositions: Journal of Asian Earth Sciences, v. 59, no. C, p. 219–230.
1054 Wang, C., Feng, Z., Zhang, L., Huang, Y., Cao, K., Wang, P., and Zhao, B., 2013, Cretaceous
1055 paleogeography and paleoclimate and the setting of SKI borehole sites in Songliao Basin,
1056 northeast China: Palaeogeography, Palaeoclimatology, Palaeoecology, v. 385, p. 17–30.
1057 Wansard, G., De Deckker, P., and Julià, R., 1998, Variability in ostracod partition coefficients
1058 D(Sr) and D(Mg): Chemical Geology, v. 146, no. 1-2, p. 39–54.
1059 Williams, D.F., Peck, J., Karabanov, E.B., Prokopenko, A.A., Kravchinsky, V., King, J., and
1060 Kuzmin, M.I., 1997, Lake Baikal Record of Continental Climate Response to Orbital
1061 Insolation During the Past 5 Million Years: Science, v. 278, no. 5340, p. 1114–1117.
1062 Winnick, M.J., Chamberlain, C.P., Caves, J.K., and Welker, J.M., 2014, Quantifying the isotopic
1063 “continental effect”: Earth and Planetary Science Letters, v. 406, p. 123–133.
1064 Wong, C.I., Banner, J.L., and Musgrove, M., 2011, Seasonal dripwater Mg/Ca and Sr/Ca
1065 variations driven by cave ventilation: Implications for and modeling of speleothem
1066 paleoclimate records: Geochimica et Cosmochimica Acta, v. 75, no. 12, p. 3514–3529.
1067 Wu, H., Zhang, S., Hinnov, L.A., Jiang, G., Yang, T., Li, H., Wan, X., and Wang, C., 2014,
1068 Cyclostratigraphy and orbital tuning of the terrestrial upper Santonian-Lower Danian in
1069 Songliao Basin, northeastern China: Earth and Planetary Science Letters, v. 407, p. 82–95.
1070 Xia, J., Ito, E., and Engstrom, D.R., 1997, Geochemistry of ostracode calcite: Part 1. An
1071 experimental determination of oxygen isotope fractionation: Geochimica et

Cosmochimica Acta, v. 61, no. 2, p. 377–382.

Xia, J., Engstrom, D.R., and Ito, E., 1997, Geochemistry of ostracode calcite: Part 2. The effects of water chemistry and seasonal temperature variation on Candona rawsoni: Geochimica et Cosmochimica Acta, v. 61, no. 2, p. 383–391.

Zhang, J., Holmes, J.A., Chen, F., Qiang, M., Zhou, A., and Chen, S., 2009, An 850-year ostracod-shell trace-element record from Sugan Lake, northern Tibetan Plateau, China: Implications for interpreting the shell chemistry in high-Mg/Ca waters: Quaternary International, v. 194, no. 1-2, p. 119–133.

Zimmerman, S.R.H., Hemming, S.R., Hemming, N.G., Tomascak, P.B., and Pearl, C., 2011, High-resolution chemostratigraphic record of late Pleistocene lake-level variability, Mono Lake, California: Geological Society of America Bulletin, v. 123, no. 11-12, p. 2320–2334.

1085 FIGURES

1086 Figure 1. Illustration of evaporation relationships used to parameterize the partial derivatives.
1087 Inset plots show regions of linear approximation assuming $F_{evap}<0.2$ within each time step (blue
1088 shading). Dashed lines are uncertainty. See text for equations describing relationships. (A)
1089 Rayleigh evaporation of $\delta^{18}O$, total (kinetic and equilibrium) fractionation, ε, is 13.5 +4.7/-3.6‰
1090 (5 to 35 °C and 50 to 90% humidity). (B) Mass conservation of solute, M (that is, Mg or Sr),
1091 with an initial lake concentration of 10 ± 2 mmol.

1092

1093 Figure 2. Illustration of mixing relationships used to parameterize the partial derivatives for
1094 volume increase. Inset plots show regions of linear approximation assuming $F_{input}<1.2$ within
1095 each time step (blue shading). Dashed lines are uncertainty. See text for equations describing
1096 relationships. (A) $\delta^{18}O$ mixing (input water of -15 ± 2‰, initial lake water of -3‰). (B) Mixing
1097 of initial concentration (10 ± 2 mmol) with a dilute input solute concentration of 3 mmol.

1098

1099 Figure 3. Illustrative Application of HyBIM to the Lake Miragoane Ostracod (*Candona* sp.)
1100 record. (A) Original $\delta^{18}O$, Mg/Ca and Sr/Ca records (grey dots) from Hodell and others (1991)
1101 and Curtis and Hodell (1993). Data are plotted on the original age model. For model input the
1102 data are kernel smoothed using an Epanechnikov kernel. The cross validated bandwidth (BW;
1103 see text for explanation) is listed for each record ($\delta^{18}O$, Mg/Ca and Sr/Ca). The solid black line is
1104 the mean and the dashed black lines are the 1σ. (B) HyBIM results for the Lake Miragoane
1105 records using partition coefficient and vital effect data from Engstrom and Nelson (1991) and
1106 Keatings (1999) derived for *Candona* sp. The red line is the empirical relationship for isotopes in

precipitation (0.26‰/°C) derived from empirical tropical GNIP stations (fig. A2; after Rozanski and others, 1993).

Figure 4. Illustrative Application of HyBIM to the Songliao Basin Ostracod (*Cypridea* sp.) Record. (A) Original $\delta^{18}O$, Mg/Ca and Sr/Ca records (grey dots) from Chamberlain and others (2013). Data are plotted on the original age model of Wan and others (2013). For model input the data are kernel smoothed using an Epanechnikov kernel from 84 to 88 Ma (densely sampled portion of the record). The cross validated bandwidth (BW; see text for explanation) is listed for each record ($\delta^{18}O$, Mg/Ca and Sr/Ca). The solid black line is the mean and the dashed black lines are the 1σ. (B) HyBIM results for the Songliao Basin record using partition coefficient data from DeDeckker and others (1999) derived for *Cyprideis* sp., the extant, closely related genus of *Cypridea* sp. The solid line is the median and the dashed blue lines are the 95% confidence interval of the Monte Carlo estimation. The approximate position of OAE 3 is denoted by the red bar, which corresponds to a peak the predicted temperature. The red line is the empirical relationship of Rozanski and others (1993) for isotopes in precipitation (0.58 ‰/°C) derived from mid-latitude Global Network of Isotopes in Precipitation (GNIP) stations.

Figure A1. Schematic of HyBIM model structure. The model structure uses a matrix inversion to solve a system of three equations ($x = \mathbf{A}^{-1}b$) implemented at each time step to calculate changes in lake volume (from the combined evaporation and inputs) and basin average air temperature. After smoothing and interpolating to an even time series, the input dataset (time series of $\delta^{18}O$, Mg/Ca and Sr/Ca from biogenic carbonate), given a set of adjustable input parameters (right side of the fig.; table 1), is first placed in lake water composition ($\delta^{18}O$, [Mg] and [Sr] Lake Water).

1130 The first derivative of the lake water time series is inputted as the b vector at each time step
1131 (d(δ^{18}O), d[Mg] and d[Sr]). The partial derivatives that make up the **A** matrix are substituted at
1132 each time step using mixing equations and evaporation equations (eqs 5 to 9 for F_{evap} and F_{input}
1133 derivatives), or estimated for temperature (the T derivatives) based on the geographic location
1134 (see text for details). For each Monte Carlo iteration the model produces a time series of the x
1135 solution vector. To provide summary statistics after combining the evaporation and lake input
1136 variables to calculate changes in volume we calculate the median and 95% range (as in figs. 3
1137 and 4).
1138
1139 Figure A2. Annual weighted precipitation δ^{18}O and mean annual temperature from the Global
1140 Network in Precipitation Data (GNIP) as compiled by the Stable Water Isotope Intercomparison
1141 Group (SWING). Following Rozanski and other (1993) we calculate slope of the temperature vs.
1142 weighted precipitation δ^{18}O for the mid and high latitude (> 23°) sites (grey), and tropics (black).
1143 We only use the empirical regression (slope and uncertainty) for the tropics in modeling of Lake
1144 Miragoane temperature changes. For the Songliao Basin we use the original regression of
1145 Rozanski and others (1993) of 0.58 ‰/°C.
1146

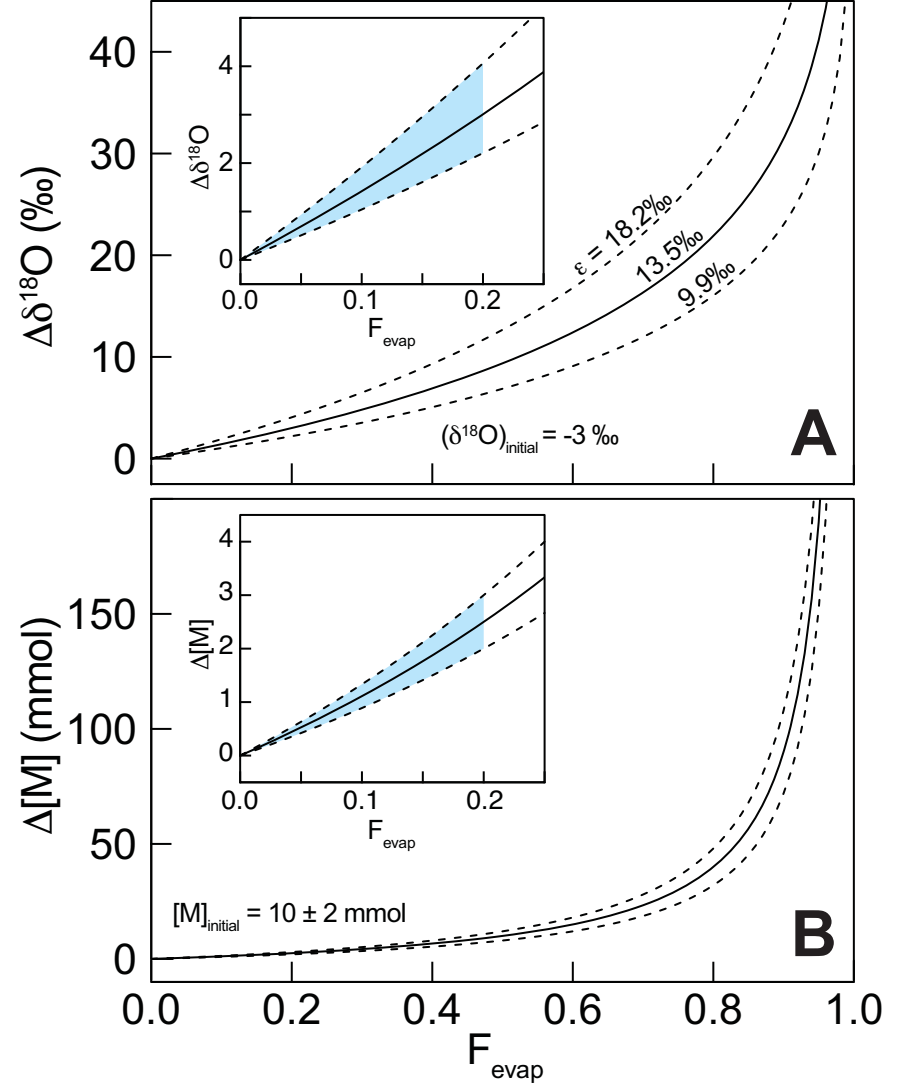
Δδ18O (‰)
40
30
20
10
0
Δδ18O
4
2
0
0.0
0.1
0.2
Fevap
ε = 18.2‰
13.5‰
9.9‰
(δ18O)initial = -3 ‰
A
Δ[M] (mmol)
150
100
50
0
Δ[M]
4
3
2
1
0
0.0
0.1
0.2
Fevap
[M]initial = 10 ± 2 mmol
B
0.0
0.2
0.4
0.6
0.8
1.0
Fevap

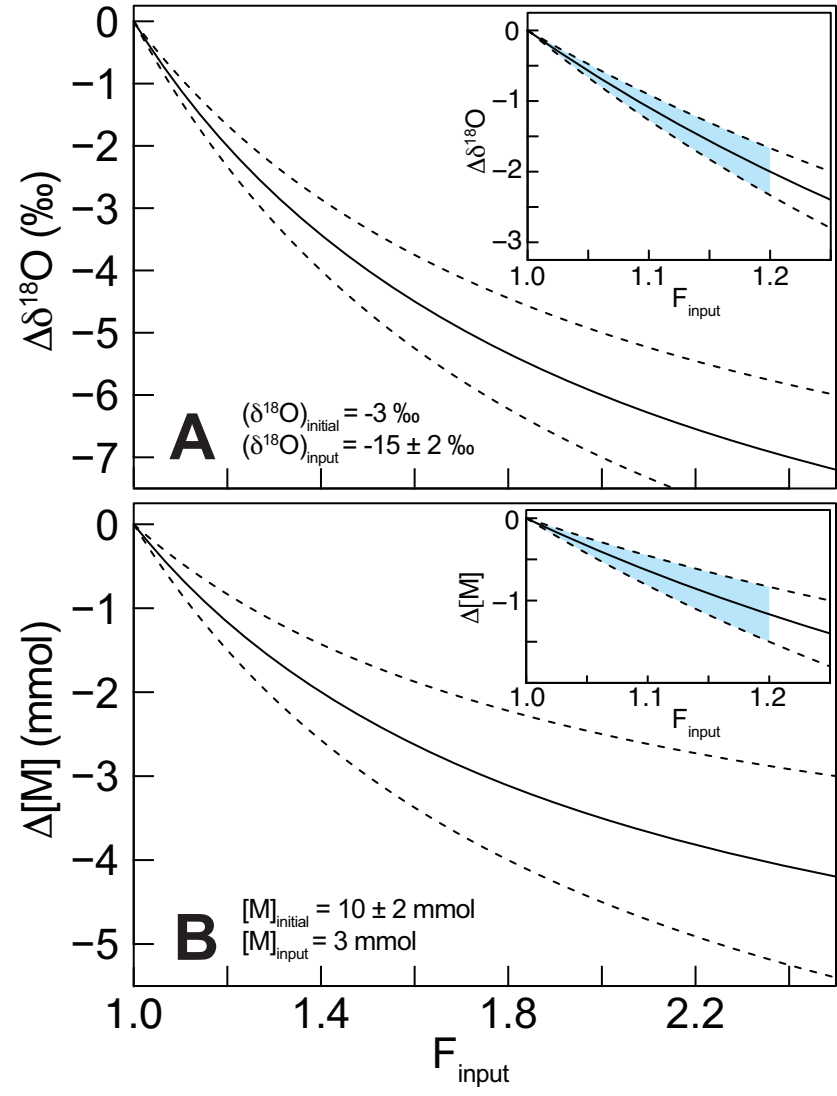
A
$(\delta^{18}O)_{initial}$ = -3 ‰
$(\delta^{18}O)_{input}$ = -15 ± 2 ‰
$\Delta\delta^{18}O$ (‰)
$\Delta\delta^{18}O$
F_{input}
B
$[M]_{initial}$ = 10 ± 2 mmol
$[M]_{input}$ = 3 mmol
Δ[M] (mmol)
Δ[M]
F_{input}

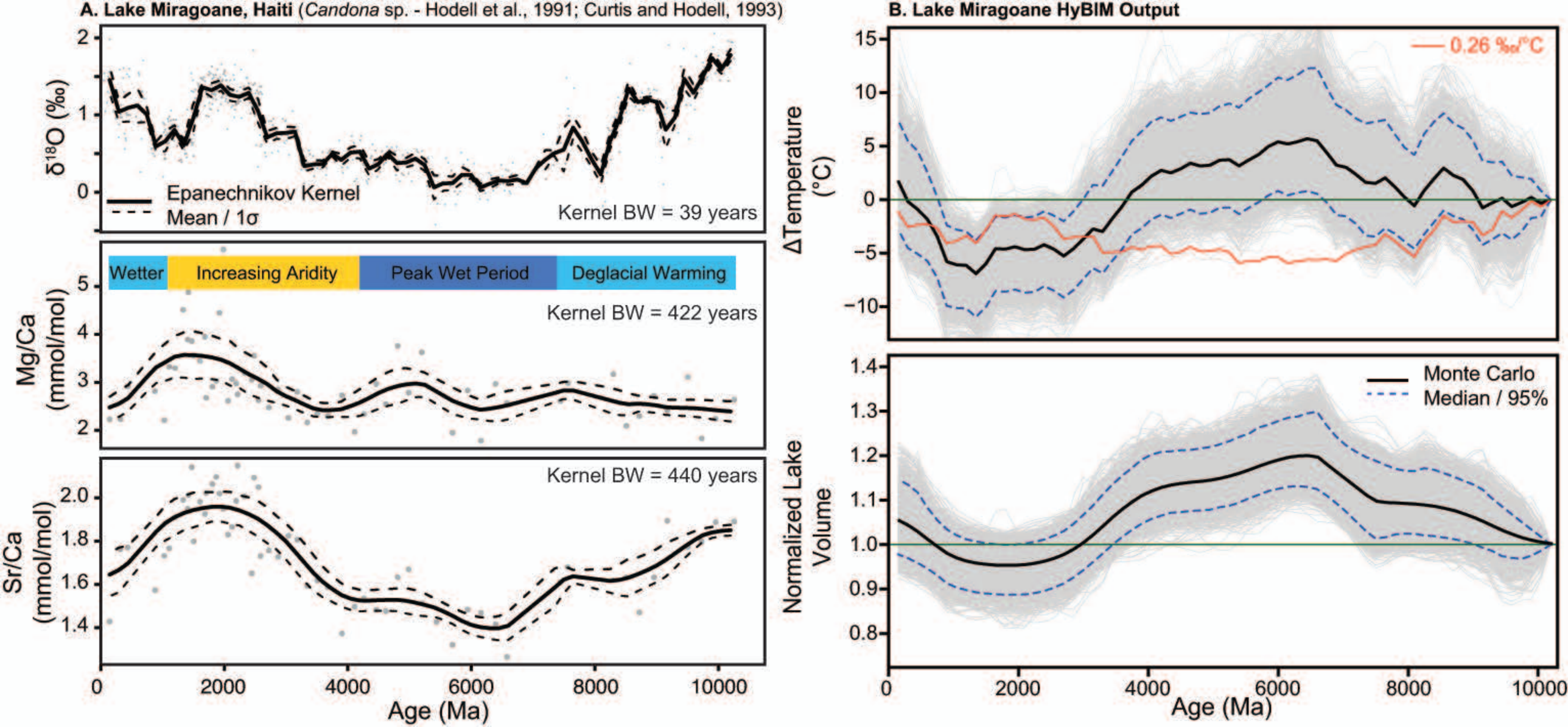
A. Lake Miragoane, Haiti (Candona sp. - Hodell et al., 1991; Curtis and Hodell, 1993)
δ18O (‰)
Epanechnikov Kernel
Mean / 1σ
Kernel BW = 39 years
Wetter
Increasing Aridity
Peak Wet Period
Deglacial Warming
Mg/Ca (mmol/mol)
Kernel BW = 422 years
Sr/Ca (mmol/mol)
Kernel BW = 440 years
Age (Ma)
B. Lake Miragoane HyBIM Output
ΔTemperature (°C)
0.26 ‰/°C
Normalized Lake Volume
Monte Carlo
Median / 95%
Age (Ma)

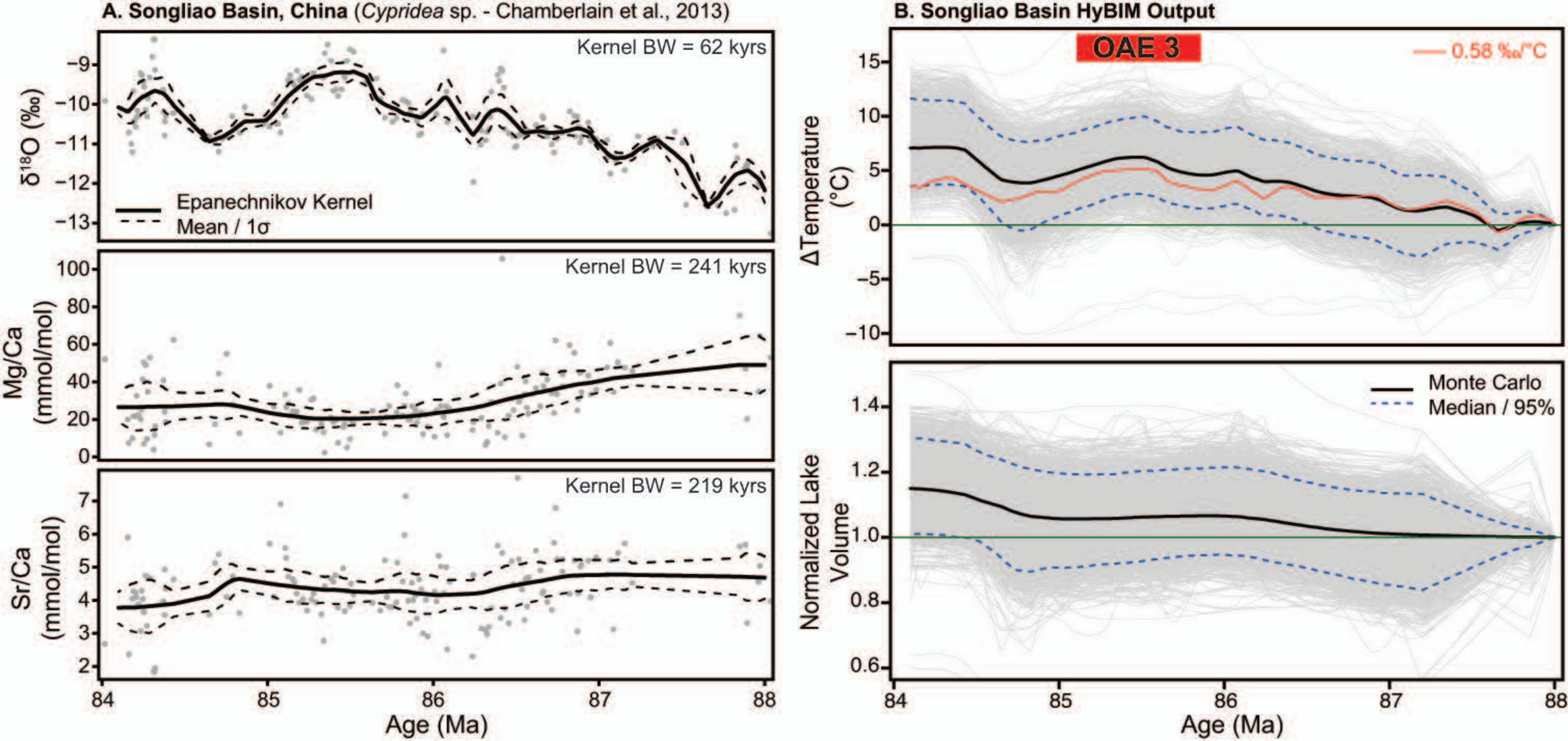
A. Songliao Basin, China (Cypridea sp. - Chamberlain et al., 2013)
Kernel BW = 62 kyrs
δ18O (‰)
Epanechnikov Kernel
Mean / 1σ
Kernel BW = 241 kyrs
Mg/Ca (mmol/mol)
Kernel BW = 219 kyrs
Sr/Ca (mmol/mol)
Age (Ma)
B. Songliao Basin HyBIM Output
OAE 3
0.58 ‰/°C
ΔTemperature (°C)
Monte Carlo
Median / 95%
Normalized Lake Volume
Age (Ma)

Input Dataset

Input Parameters

$\delta^{18}O$ Record

Sr/Ca Record

Mg/Ca Record

K_D[Mg], K_D[Sr]

$\delta^{18}O$ Vital Effect

Lake [Ca]

Temperature

Humidity

Stream [Sr], [Mg] and $\delta^{18}O$

Kernel Smoothed Mean and Residuals

Interpolate to Evenly Spaced Time Step

Place in Lake Water Composition

$\delta^{18}O$ Lake Water

[Sr] Lake Water

[Mg] Lake Water

Calculate Evaporation Derivates (F_{evap})

Calculate Mixing Derivates (F_{input})

Take First Derivate of Lake Water Timeseries

$d(\delta^{18}O)$

d[Sr]

d[Mg]

$$\begin{bmatrix} \frac{\partial(\delta^{18}O)}{\partial T} & \frac{\partial(\delta^{18}O)}{\partial F_{evap}} & \frac{\partial(\delta^{18}O)}{\partial F_{input}} \\ \frac{\partial[Sr]}{\partial T} & \frac{\partial[Sr]}{\partial F_{evap}} & \frac{\partial[Sr]}{\partial F_{input}} \\ \frac{\partial[Mg]}{\partial T} & \frac{\partial[Mg]}{\partial F_{evap}} & \frac{\partial[Mg]}{\partial F_{input}} \end{bmatrix}^{-1} \times \begin{bmatrix} d(\delta^{18}O) \\ d[Sr] \\ d[Mg] \end{bmatrix} = \begin{bmatrix} dT \\ dF_{evap} \\ dF_{input} \end{bmatrix}$$

Partial Derivatives

Solution

Solve for dT, dF_{evap} and dF_{input} for each time step

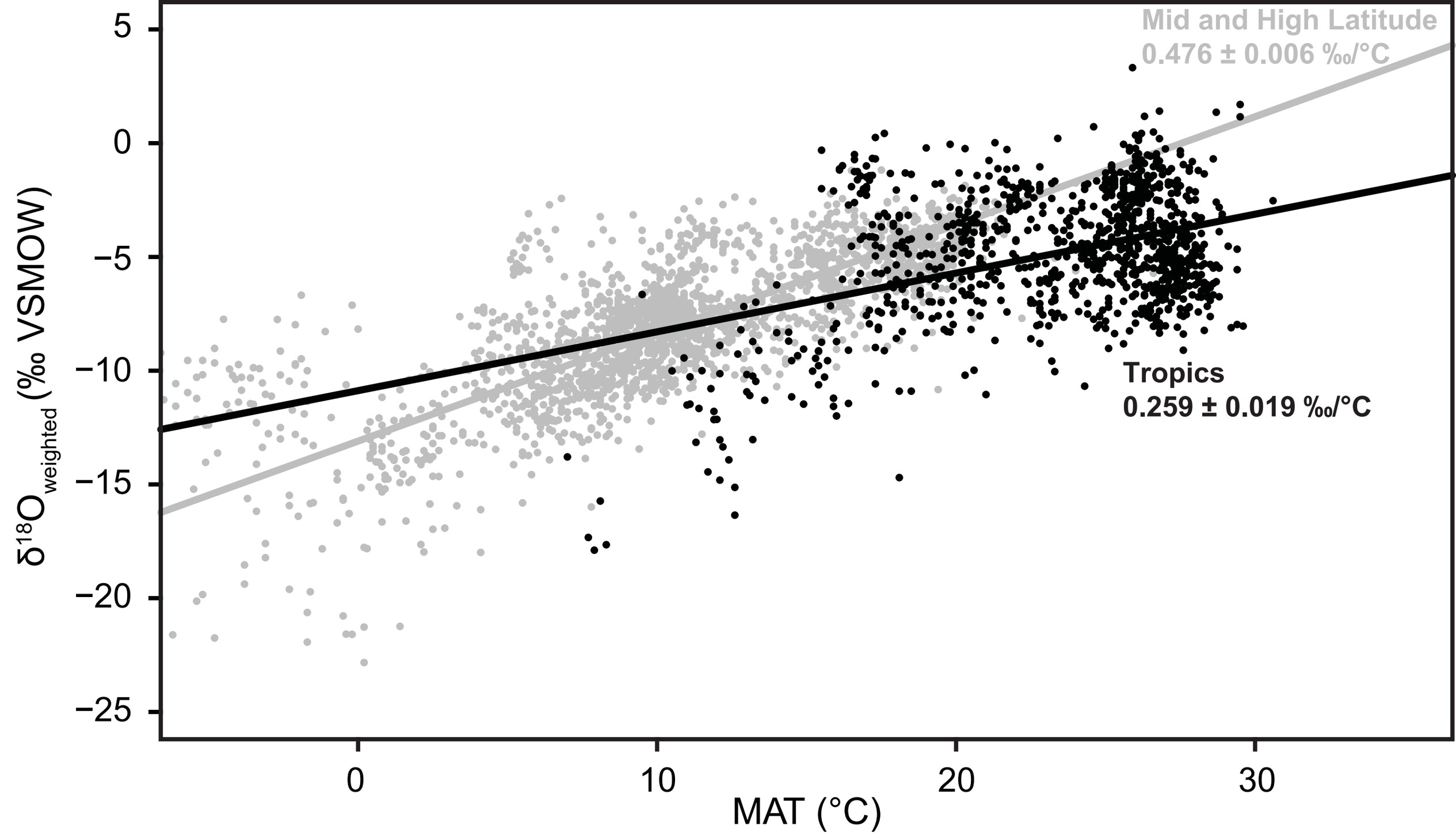
Mid and High Latitude
0.476 ± 0.006 ‰/°C
Tropics
0.259 ± 0.019 ‰/°C
δ18Oweighted (‰ VSMOW)
MAT (°C)
5
0
−5
−10
−15
−20
−25
0
10
20
30